THERMOMECHANICAL PROCESSING AND CONSTITUTIVE STRENGTH OF HOT ROLLED MILD STEEL

BY

SEKUNOWO, Israel Olatunde
B.Tech (Hons. Akure), M.Sc (Lagos)

Department of Metallurgical and Materials Engineering
University of Lagos, Nigeria

JULY 2010

THERMOMECHANICAL PROCESSING AND CONSTITUTIVE STRENGTH OF HOT ROLLED MILD STEEL

BY

SEKUNOWO, Israel Olatunde
B.Tech (Hons. Akure), M.Sc (Lagos)
(979004091)

Thesis Submitted to the School of Postgraduate Studies, University of Lagos in partial fulfillment of the requirements for the degree of Doctor of Philosophy

In

Mechanical Metallurgy

Department of Metallurgical and Materials Engineering
University of Lagos, Nigeria

JULY 2010

SCHOOL OF POSTGRADUATE STUDIES
UNIVERSITY OF LAGOS

CERTIFICATION

This is to certify that the Thesis:

THERMOMECHANICAL PROCESSING AND CONSTITUTIVE STRENGTH OF HOT ROLLED MILD STEEL

Submitted to the
School of Postgraduate Studies
University of Lagos

For the award of the degree of
DOCTOR OF PHILOSOPHY (Ph.D.)

Is a record of original research carried out

By

SEKUNOWO, Israel Olatunde
Department of Metallurgical and Materials Engineering

------------------------------------	--------------------	---------
AUTHOR'S NAME	**SIGNATURE**	**DATE**
------------------------------------	---------------------	---------
1ST SUPERVISOR'S NAME	**SIGNATURE**	**DATE**
------------------------------------	------------------------	---------
2ND SUPERVISOR'S NAME	**SIGNATURE**	**DATE**
-------------------------------------	--------------------	---------
3RD SUPERVISOR'S NAME	**SIGNATURE**	**DATE**
-------------------------------------	--------------------	--------
INTERNAL EXAMINER	**SIGNATURE**	**DATE**

INTERNAL EXAMINER	**SIGNATURE**	**DATE**
SPGS REPRESENTATIVE	**SIGNATURE**	**DATE**

UNIVERSITY OF LAGOS

UNIVERSITY
OF LAGOS

DEDICATION

This work is dedicated to the glory of God, the custodian of knowledge, wisdom and understanding.

ACKNOWLEDGEMENTS

Foremost, I give glory to God Almighty who has enabled me in every way to carry out this study. I am eternally grateful to my supervisor Professor S.A. Balogun for his unquantifiable contribution, guidance, concern, promptness and wealth of experience he brought to bear on timely and successful completion of the work. The contribution of my second supervisor Dr. G.I. Lawal (Associate Professor) is tremendous. He is highly supportive and always ready to make sacrifices towards the timely completion of the research.

I am really encouraged by the robust support offered by Professor D.E. Esezobor, the Head of Department of Metallurgical and Materials Engineering whose contributions have in no small measure added value to the quality of the work.

My third supervisor, Dr. S.O. Adeosun contributed immensely too to the successful completion of the work. His offer to peruse every draft before I passed same to my supervisors actually facilitated the rapid progress made during the study. My grateful thanks are due to the management of Universal Steels Limited, Ikeja for allowing me the use of their facilities during the industrial phase of experimentation. I also appreciate the assistance rendered by staff of Metallurgical and Materials Laboratory, University of Lagos.

I am highly indebted to my colleagues who wholeheartedly encouraged and supported me; Dr. J.O. Agunsoye, Engr. Mrs. E.F. Ochulor, Engr. Mrs. C.U. Kuforiji, Engr. W.A. Ayoola and Mr. Gbeminiyi Sobamowo. The contribution of my bosom friend Professor G.A. Odeshi, Department of Mechanical Engineering, University of Saskatchewan, Canada cannot be quantified. He made available most of the materials used for the literature review. I am not under any illusions that I would have taken upon myself the task of pursuing a doctoral research without the cooperation, patience and love of my wife Christiana Sekunowo and my children; Toyin, Olumide, Bukola, Bunmi and Pelumi. May God bless all abundantly, amen.

UNIVERSITY OF LAGOS

ABSTRACT

This work examined thermo-mechanical and metallurgical parameters (temperature and cooling rate) that give rise to substantial improvement in the basic functional strength characteristics of high-yield reinforcing steels produced in a conventional mill. A new process tagged Temperature Tracking-Jet Water Spray (TT-JEWAS) was developed to achieve requisite in-process control of thermal variations on one hand and fast undercooling by spray quenching on the other. The alternative microstructure obtained, lower bainite instead of pearlite induced in the steel, gave rise to a significant improvement in the strength characteristics (Yield strength, 422-843MPa; Ultimate tensile strength, 704-

1173MPa, Impact energy, 85-111J) and reliability of the steel. These compared favourably with both local and international standards (NIS 117:2004, BS 4449:1988 and ASTM A615: 1996). This result implies that substantial import substitution can be achieved in the high-yield reinforcing steel bar industry to give tremendous boost to the nation's Gross Domestic Products (GDP). Bainitic Yield strength-band and Empirical model developed from the results of this work are extremely useful for in-process quality control and prediction of yield strength of hot rolled steel bars. This will lead to improvement in processing methods in the local steel industry.

UNIVERSITY OF LAGOS

TABLE OF CONTENTS

LIST OF FIGURES

LIST OF PLATES

LIST OF TABLES

CHAPTER ONE

1.0 INTRODUCTION

1.1 Background of the study

Steel is one of the most important engineering materials due to its superior cost/performance ratio. Though faced with stiff competition from other materials, steel remains the basis for measuring the level of a nation's technological advancement. Similarly, the quantity of steel products consumed by the citizens of a country is indicative of the level of civilization subsisting in the country. The most important characteristics of steel are its mechanical properties of which the strength factor plays a vital role. Engineering strength is assessed in terms of yield strength (σ_y), tensile strength (σ_E), modulus of elasticity (E), impact toughness (I) and hardness (H).

The yield strength however, is the principal index of the mechanical characteristics of any metal. This is because yielding of ductile material such as steel produces permanent deformation. Hence, any increase in the strength of a metal increases the reliability and service life of the structure (machine) in which it is used. On the other hand, the consequences of low strength characteristics often give rise to short life span, warpage, undesirable deflection and even failure or collapse.

Hot rolled mild steel bars with carbon in the range of 0.1-0.3% are the most preferred among different grades of carbon steels used in everyday engineering applications (ASTM 1996). Mild steel constitutes the bulk (90% by wt.) of all structural steel profiles (bars, angles, channels, I-beams and H-beams) commonly employed in construction and allied engineering works. The steel possesses excellent formability and is easily fabricated at a relatively low cost. This grade of steel also exhibits excellent welding characteristics without impairment of structural integrity after welding. In view of these desirable properties of mild steel, its use continues to grow at a rapid pace in today’s technology. Other areas of mild steel applications include automotive, foundry and agricultural mechanization equipment.

Construction mild steel bars can be produced through hot rolling in a conventional or a compact mill. Typical processing methods for the production of rolled steel bar in a conventional mill entails charging of rolling stocks (billets or ingot) into a reheat furnace and allowing it to attain the rolling temperature (1000^0-1200 C). This is followed by sequential introduction of the billets into the rolling stands, which are usually arranged in tandem for plastic deformation culminating in the desired profile (rod, beam, channel angle, etc) and allowing them to cool in air. In contrast, compact mill operations are highly integrated, involving direct feeding of the rolling mill with billets from a continuous caster. The process is highly flexible in terms of control and monitoring of processing variables namely temperature, strain rate and microstructural transformation in the final product. Improved mechanical properties of the rolled bars are achieved by the combination of these processing conditions. This is the current status of a modern mill through which many grades of special quality steels are efficiently rolled to good metallurgical, dimensional and surface conditions.

Most mills in the developing world especially Africa, still operate on the basis of conventional rolling. The operations are usually devoid of controlling and monitoring of relevant processing variables (temperature, strain rate and cooling rate). Proper control of these variables will ensure that the desirable microstructure is evolved in the final product. Steel bars produced through conventional rolling often exhibit abysmally low mechanical properties. This is because the versatility of steel in terms of its very high mechanical properties is derived from the nature of its microstructure (Llewellyn, 1992).

Given the increasing global demand for steel bars of superior strength characteristics at low cost, decades of research have thrown-up various methods by which this problem could be addressed. Two of these methods relevant to the present study are chemical composition modification and process control. However, the high cost of composition adjustment makes the approach unattractive. Rather, the application of the combination of systems of Controlled Rolling (CR) and Controlled Cooling (CC) proves to be the best option (Augusti, 1998). This system however, requires some variations in processing parameters to suit individual plant production peculiarities.

Process control concept encompasses both CR and CC processes. It is aimed at improving the mechanical properties of hot rolled steel bars through the use of optimum hot rolling conditions that will give superior mechanical properties. These conditions are appropriate rolling stock composition, rolling process dynamics (temperature and strain rate) and cooling regime employed. Controlled rolling entails technological innovations, deployment of modern equipment within the rolling facility and in-process monitoring. On the other hand, Controlled cooling is a thermomechanical strengthening technique aimed at achieving desirable microstructural evolution through various phenomena namely grain-size refinement, strain hardening, solid-solution transformation and precipitation hardening. All these phenomena create in the microstructure substantial impediments to dislocation motion, which give rise to improved strength characteristics (Elmer, et al. 1989).

Solid solution hardening principle was employed in the development of Tempcore and Thermex processes. Both processes were developed and patented in the mid-eighties to meet the challenge of low strength characteristics prevalent in conventional hot rolled mild steel bars (Markan, 2004). The processes employ the principle of martensitic transformation through drastic cooling of hot rolled steel bars immediately after the finishing stand. However, industrial isothermal transformation of austenite to martensite in mild steel requires a critical cooling rate up to 500 ^{0}C/s and must be accomplished within a few seconds. This is often difficult to achieve. Thus, Tempcore and Thermex processes are fraught with four major constraints that have made their adoption difficult (Bontcheva and Petzov, 2005). These constraints include high cost, need for plant re-engineering, limited scope of product applicability and patent whereby the process operating variables are not published due to patent restrictions.

One of the efficient and cost effective means of achieving improvement in the mechanical properties of conventional hot rolled steel bars may therefore, be found in developing an alternative microstructure of which the grains play a major role without re-engineering of production processes.

The microstructure of steel bars produced in conventional mill comprises ferrite and pearlite while bars from compact mill usually exhibit a dual-phase structure of martensite-pearlite. The formation of martensite however, requires enormous drastic cooling rate, which is practically difficult to achieve in mild steel (Vijendra, 2004).

Alternatively, a well controlled fast cooling of austenite could be effected such that a different microstructure is formed. This can be achieved through what can be described as a middle course critical cooling rate, which is between drastic quenching as obtained in martensitic hardening and air-cooling as in conventional rolling. In a bid to overcome some of the foregoing constraints and challenges, attempt is made in this study to develop a new microstructure consisting of Lower Bainite (LB) in hot rolled mild steel bar through spray-quenching (SQ) on the cooling bed.

Lower bainitic steels (LBS) have widespread applications as structural members in bridges, cranes and other structures (Arvedi and Guidani, 2004). The high strength properties of LBS are due to the interstitial atoms of carbon and the high dislocation density in the α-martensitic phase (Henkel and Pence, 2002). The formation of inclusion of dispersed carbides in the α- solid solution is responsible for high hardness, strength and ductility of LBS. Development of bainitic structure in mild steel through spray quenching is favoured above martensitic structure for reasons of lower cost and the virtual elimination of retained austenite after transformation. Retained austenite in eutectoid steel is reported to be a precursor to ageing (Raghavan, 2006).

This work examines the challenges above and proffers solutions that are scientific, practical and cost effective. The process variables established in the study will enable the production of reinforcing steel bars with strength characteristics comparable to international standards.

1.2 Statement of the Problem

The incessant failure/collapse of structures such as buildings and bridges across the country is attributed to the use of substandard materials particularly reinforcing steel. This is due to the abysmally low strength characteristics of conventional hot rolled high-yield steel bars, which persist in the steel industry of the developing countries including Nigeria (Table 1.1). Consequences of inadequate strength characteristics often manifest in warpage, excessive deflection and even failure/collapse leading to loss of lives and property (Balogun, et al. 2009).

Table 1.1Standard strength specifications for high-yield steel bar

Strength Parameters (MPa)	Standard Specifications			Reinforcing Steel Status (Nigeria) (Balogun, et al. 2009)
	NIS 117:2004	BS 4449:1988	ASTM A615:1996	
Yield Strength	420	460	414	300-380
Ultimate Tensile Strength	500	600	600	400-500
Impact Energy (J)	80-120	80-120	90-130	50-70

Usually the strength characteristics of hot rolled constructional high-yield steel bar are determined by such factors as (a) production history of the rolling stock in terms of the charge make-up (b) metallurgical phenomena taking place during hot rolling and (c) cooling regime of the final product. However, two processing parameters, temperature and cooling rate are critical in conventional mill operations. Finding the appropriate method of strength improvement compatible with plant peculiarities requires in-depth knowledge of hot rolling dynamics and metallurgical reactions involving microstructural transformations during the process of hot rolling. The interplay of these two parameters influences the mechanical properties of the steel bar. This research investigates these parameters and the properties they confer on hot rolled high-yield steel bars. The work is carried out based on two main processing parameters namely temperature (finishing) and varied fast cooling rates through spray quenching.

1.3 AIM AND OBJECTIVES

The main aim of this study is to solve the problem of low strength characteristics prevalent in conventional hot rolled mild steel bars. The specific objectives are to:

(a) Establish appropriate range of finishing temperatures amenable to the development of microstructure that confer improved strength.

(b) Establish suitable range of cooling rates that induce alternative microstructure for improved mechanical properties.

(c) Develop alternative microstructure to replace the conventional pearlite in the rolled steel bar.

(d) Develop an in-process technique suitable for industrial use to improve quality control of steel bar production.

1.4 Scope of Study

This research covers all construction high-yield steel bars of NST 42/50HD within the size range Ø12mm-32mm and its equivalents (BS 970, AISI 1030). Improvement in the engineering strength characteristics namely yield strength, ultimate tensile strength, impact toughness and hardness is top priority of the study. The yield property band and the corresponding empirical model developed are applicable only to the category of sizes of steel bars covered by this study in the as-rolled conditions.

1.5 Significance of the Study

There is a growing demand for reinforcing steel bars of high quality in order to meet the demand for complex structural designs and safety. The efficiency and cost effectiveness of the method employed to accomplish substantial improvement in the strength characteristics of steel bars provide opportunity of growth for the local steel industry. Specifically, this research provides for:

(i) Restoration of confidence in the local reinforcing steel bars, which will lead to improved patronage, reduction in importation and increase in the Gross Domestic Product (GDP).

(ii) The establishment of relevant hot rolling process variables (thermal and cooling rates) which give rise to improved processing method in the local steel industry.

(iii) Production of reinforcing steel exhibiting markedly improved strength for value addition.

(iv) The establishment of technological, metallurgical and thermomechanical variables for effective control of hot rolling process thus extending the frontier of knowledge.

1.6 Research Justification

One of the major causes of incessant collapse of structures such as buildings and bridges is the use of substandard materials particularly reinforcing steel. This often gives rise to loss of lives and property and huge economic loss. In Figure 1.1, it is observed that the ratio of local production of steel bars to importation is 1:3 for each of the three years, 2006, 2007 and 2008. Improvement in the strength characteristics of the locally manufactured steel bars will lead to increase patronage hence reduction in importation. There will also be increase in the local plant installed capacity utilisation which is currently 30%.

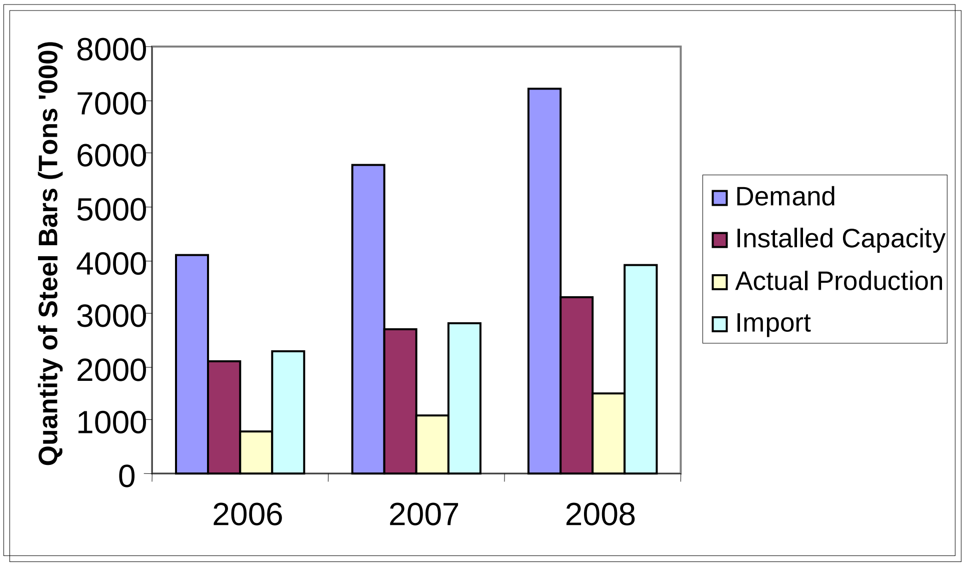

Figure 1.1: Tonnage of Construction Steel Bars' Demand, Production and Import in Nigeria (Steelman Group of MAN)

1.7 RESEARCH QUESTIONS

The questions below will provide the pathway to this research.

- What are the factors militating against the attainment of high quality rolled products at competitive cost?
- What are the current hot rolled product strength improvement techniques?
- How can a new microstructure be induced in hot rolled steel bar that confers markedly improved strength characteristics?
- By what mechanism can alternative microstructure be induced in rolled steel at competitive cost?

1.8 OPERATIONAL DEFINITION OF TERMS

For the purpose of this study, the following terms are defined as follows:

Austenite

An interstitial solid solution of 1.7% carbon (maximum) in face-centred cubic (fcc) iron.

Bainitic structure

Bainite is a non-laminar mixture of ferrite and aggregates of carbide formed in low carbon steel at cooling rates faster than air-cooling. Two types of bainite are feasible based on transformation temperature. The upper bainite structure usually evolved just below 450 ^{0}C. The structure is unstable and resembles pearlite. Lower bainite, on the other hand, forms in the temperature range of 400–250 ^{0}C resulting in non-laminar structure but precipitates of carbide in ferrite matrix. Hence, the mechanical properties of lower bainite are better than those of upper bainite and pearlite.

Bar

A bar is a long rolled rod (plain or ribbed) product of size in the range 10-32 mm in diameter.

Constitutive strength

Constitutive strength is the measure of a material's resistance to deformation/failure based on its microstructural conditions.

Ferrite

Ferrite is the structure formed as a result of limited interstitial solid solution of carbon in body centred cubic iron. There are two variants of ferrite namely **α-ferrite** formed at room temperature to 910 ^{0}C with maximum solubility of carbon of 0.02 wt % and **δ-ferrite** from 1394-1539 ^{0}C of 0.09 wt % maximum carbon solubility. These conditions account for the soft and relatively large amount of ductility usually exhibited by ferrite.

Martensite

Martensite is a supersaturated solid solution of carbon in iron. Its formation in plain carbon steel is by a diffusionless shear transformation on a very rapid cooling of austenite. The strength of steel increases as the volume fraction of martensite increase while the toughness decreases hence, the imperative of martensite tempering for enhanced usefulness.

Pearlite

A composite mixture of ferrite and cementite (Fe_3C) due to eutectoid reactions of austenite feasible only in hypo eutectoid steels. Cementite is hard and brittle. Its level of hardness is determined by the carbon concentration. The texture of pearlite consists of alternate platelets of ferrite and cementite. The inter lamina spacing between the plates usually determines the grain size and to a large extent influences the mechanical properties.

Quenching

The sudden cooling of a material from high temperature to room temperature. It represents a major form of fast under cooling at competitive cost. Water has been established as the most versatile of all industrial quenchants.

Rolling Stock

A cast steel material in form of billet or ingot that is used as the work-piece in rolling.

Strength

Strength is a measure of resistance to external applied force which tends to cause deformation and/or failure. The force acting may be tensile, compressive or torsional in either static or dynamic environment.

Thermo-mechanical processing

A simultaneous high temperature plastic deformation. It is one of the major conventional shaping methods where the working stock is heated to 0.6 of its melting point. At this temperature, the material is substantially free from strain hardening. The process also allows the inducement of desirable microstructure, which affects the properties of the final product.

Tramp

A tramp is an extremely refractive and undesolved object in molten steel. Tramps have the capacity to distort microstructural integrity of cast rolling stocks, which are carried over to the rolling process and eventually into the rolled products thereby impairing the mechanical properties.

CHAPTER TWO

2.0 LITERATURE REVIEW

The challenge posed by the characteristic low strength of conventional hot rolled mild steel bars used for concrete reinforcement is of global concern. This is because most structural failures resulting in loss of lives and property are partly attributable to the use of substandard reinforcement. From literature (Bowering, (1968), Fapiano, et al. (2001), Bai, et al. 2003) and other relevant empirical studies (Markan, 2004, Hiroshi, 2007, Balogun, et al. 2009), it is established that major factors causing this problem can be metallurgical and process dysfunctions. Metallurgical conditions entail the chemical composition of rolling stocks and microstructural evolution in rolled products. Chemical composition adjustment in term of microalloy addition has proved to be unattractive for reason of high cost (Owen and Knowles, 1992). In the absence of micro-alloy additions to the rolling stock, the other viable and cost effective possible remedy to the phenomenon of low strength can be found in microstructure development through innovative approach to the hot rolling process. Hence, the need to examine in-depth the characteristic strength of mild steel bars in relation to the chemical metallurgy of the rolling stock (mild steel billet), thermal variations during rolling as it affects strain-rate and the resulting microstructure of the hot rolled steel bar.

2.1 Chemical Metallurgy of Construction Steel Rolling Stock

The production history of rolling stock (billet/ingot) impacts on the rolling process on one hand and influences the mechanical properties of the product on the other. The control of elemental concentrations and internal cleanness given by the level of deoxidation and the quanta of inclusions are imperative.

2.1.1 Rolling Stock Elemental Composition

The control of composition of mild steel within acceptable tolerance limits is an important requirement for the production of hot-rolled steel bars of desirable strength characteristics (Mamadou, et al, 2009). Presently, there is inadequate information on the actual behaviour of reinforcing steel bars produced from heterogeneous metal scraps.
This has greatly endangered many new materials with highly modified structures produced in most developing countries (Charles and Mark, 2002). Typical mild steel stock composition consits of varied concentrations of carbon, silicon, manganese, sulphur, phosphorus, iron and other trace elements such as nickel, copper, vanadium and chromium.

Tasuro, et al (2001) established that carbon is indispensable for increasing strength of steel type amenable to thermo-mechanical treatment. The ASTM A615 (1996) standard specified 0.18-0.30 percent carbon in rolling stock meant for structural purposes. However, billets of carbon concentrations below the range of 0.20-0.30 percent usually do not exhibit meaningful microstructural changes during solution treatment.

Tables 2.1 and 2.2 contain the chemical composition specifications based on cast analysis of billets meant for concrete reinforcement as published in the British standard, BS 4449 (1988) and the Nigerian Industrial Standards, NIS 117 (2004) respectively. The values specified in both tables have been harmonized with ISO 6935 parts II and I.

Table 2.1 Chemical Composition of Rolling Stock (BS 4449)

Element	Grade 250 (%Max)	Grade 460 (%Max)	Maximum Deviation Allowed (%)
Carbon	0.25	0.25	0.02
Sulphur	0.060	0.050	0.005
Phosphorus	0.060	0.050	0.005
Nitrogen	0.012	0.012	0.001

Note**:**

1. Grades are given in terms of the minimum yield strength.

2**.** Grades 460 and 250 are used for hot rolled high yield deformed and low yield plain bars respectively.

Table 2.2 Chemical Composition of Rolling Stock (NIS 117.2004)

Element	Grade 230 (%Max)	Grade 420 (%Max)	Maximum Deviation Allowed (%)
Carbon	0.25	0.25	0.02
Phosphorus	0.05	0.05	0.005
Sulphur	0.05	0.05	0.005
Copper	0.25	0.25	-
Nitrogen	0.012	0.012	0.001

Note**:** Grades 230 and 420 are used for hot rolled plain and high yield deformed bars respectively.

Good reinforcement steel must not contain sulphur and phosphorus in excess of 0.05 per cent. This is to curtail their peculiar deleterious effects on the mechanical properties of the steel. Obikwuelu (1987) demonstrated that metallic inclusions give rise to the anisotropic properties of hot rolled steels. As these inclusions get elongated during rolling, directional properties ensued. Thus, ductility and toughness are lowered in the directions normal to the rolling direction. To obtain uniform mechanical properties in all directions, the sulphur and oxygen contents must be reduced as much as possible. Similarly, any inclusions present must be small and equiaxed or globular.

Structural steels are required to exhibit good welding characteristics to guarantee the integrity of the weldment in service (Hiroshi, 2007). The concept of carbon equivalent Ceq, was introduced in order to control carbon concentrations to meet weldability criterion and strain hardening behaviour of rolling stocks. The weldability of steel is the ease with which it can be welded without complications or recourse to any special welding method. Carbon equivalent value, Ceq, for plain carbon steel (Oelmann and Davis, 1983) is usually expressed in the form:

$$Ceq = C + \frac{Mn}{6} + \frac{Cr + Mo + V}{5} + \frac{Ni + Cu}{15} \qquad 2.1$$

Where C, Mn, Cr, Mo, V, Ni and Cu are the chemical symbols for carbon, manganese, chromium, molybdenum, vanadium, nickel and copper respectively.

The range of Ceq value (equation 2.1) obtained for each melt-cycle automatically places the steel in the class of weldable or non-weldable. According to BS 4449: 1988 for weldable steel, Ceq $\leq$ 0.51 while Ceq > 0.51 is for non-weldable steel. Table 2.3 is a compilation of the average chemical composition of billets used for high yield deformed bars by the Nigerian steel manufacturers.

Table 2.3 Chemical Composition of Billets Produced in Nigeria (Balogun, et al, 2009)

Steel Producer	Elements (%)											
	C	Si	S	P	Mn	Ni	Cr	Mo	V	Cu	Fe	Ceq
Federated	.266	.164	.019	.018	.637	.026	.025	.502	.001	.220	98.626	.40
Sankyo	.209	.203	.048	.036	.876	.096	.119	.019	.003	.266	98.125	.41
Delta	.358	.397	.019	.027	1.109	.061	.077	.013	.001	.141	97.218	.58
Major	.354	.365	.037	.033	.801	.108	.118	.017	.003	.291	97.873	.54
Universal	.345	.239	.032	.029	.699	.080	.128	.019	.002	.232	98.195	.51
African	.332	.210	.036	.031	.857	.101	.105	.013	.003	.240	77.969	.52
Spanish	.376	.062	.042	.005	.587	.034	.024	.014	.011	.223	98.633	.51

With reference to Table 2.3, the Ceq values above 0.51 are 3 out of 7 for the steel production facilities investigated. The implication is that about 43% of hot rolled steel bars produced in Nigeria are non-weldable and therefore not compliant with the standards.

There is also the need to control the concentrations of other elements within acceptable limits as their presence influence the behaviour of rolled products in service. For example, copper (Cu) above 0.25 percent by weight often results in complex compounds that impair the mechanical properties of the steel.

Silicon (Si) must be restricted to the range of 0.15-0.30 percent to avoid undesirable graphitisation at the expense of cementite which may impair ductility. Manganese (Mn) enhances strength as it promotes austenite stability for desirable microstructural transformation. However, manganese performs this function effectively in plain carbon steel when present in the range 0.60-1.20 percent (Prasun and Shuhbrata 2007). Other elements such as vanadium, nickel and tin are usually limited to trace quantities.

2.1.2 Rolling Stock Internal Cleanness

The production of molten mild steel starts with the characterisation of the charges (see Figure 2.1). However, its overall quality depends on the sulphur and phosphorus contents, degree of deoxidation and level of cleanness. Steel cleanness has to do with minimizing the size and frequency of undesirable non-metallic inclusions.

a b c d

Figure 2.1 Major charges for rolling stock molten steel production

(a) Steel scraps (b) Ferro-Silicon (c) Limestone (d) Ferro-Manganese

Ghosh, et al, (2007) established that the presence of small inclusions limits the ultimate stresses attainable, >700 MPa and other desirable mechanical properties of mild steel. Only a slim allowance is usually considered for trace elements such as Zn, Sn, and Pb. These elements have a way of negatively affecting the creep strength, ductility, susceptibility to corrosion and hot workability of mild steel (Randall, 2006). Deoxidation may be achieved by oxygen lancing or via the relatively new slag foaming technique developed by Sahajwalla, et al, (2006). Steel with a high level of dissolved gases particularly oxygen and nitrogen, if not controlled by addition of small elements that have affinity for them to float out of the liquid steel at high temperature, can behave in a brittle manner (Owen and Knowles, 1992). These parameters and the influence of slag composition usually impart tremendous influence on both the microstructure and the mechanical properties of rolled product (Kitamura and Okohira, 1992).

Technology exists for rapid, sensor-based, real-time analysis of sulphur, silicon, slag and steel-oxygen activity (Ahlborg, 1997). Hence, their effective monitoring within limits is taken care of by a melting facility that has relevant sensors installed. However, production of billets in the local steel industry is carried out in various melting facilities ranging from induction furnaces to Electric Arc Furnaces (Figure 2.2). Such furnaces lack in-process control and monitoring devices.

Figure 2.2 Electric Arc Furnace (EAF)

Table 2.4 contains the average tramp elements in the charge-mix of local steelmaking facilities in comparison with the allowable values in good quality hot rolled mild steel.

Table 2.4 Tramp elements concentrations in melt charges (Balogun, et al, 2009)

Facility	Charge mix	Tramp Elements **(%)**	Allowed Conc.	Cleanness

		Cu + Sn + Zn	%Max.	Status
Sankyo	100% Steel scrap	0.50	0.46	Poor
Universal	100% Steel scrap	0.46	0.46	Satisfactory
Federated	100% Steel scrap	0.52	0.46	Poor
African	100% Steel scrap	0.47	0.46	Fair
Delta	20% Scrap + 80%DRI	0.28	0.46	Good

It is evident from Table 2.4 that most steel plants in Nigeria have high scrap input compared with the use of virgin charges represented by Direct Reduced Iron (DRl) and briquettes. The billets cast are hardly suitable for the production of long products such as rods, bars, beams and channels. However, this condition can be improved through dilution of substantial amount of virgin charges.

The data in Table 2.4 clearly show that the combination of scraps and virgin charges gives cleaner steel as in the case of Delta steel. Young (1988) reported the development of a process route for the production of low carbon, aluminum- killed steels with cleanness index of 1.5 mg/10 kg of steel and total oxygen content of 27ppm.

With optimum control of the complete production process, the desirable billet composition can be achieved through either EAF or BOF route. Owen and Knowles (1992) recommend as the best, silicon semi-killed BOF steel for use as rolling stock to produce steel bars for concrete reinforcement. However, the cost effectiveness of either of the production routes depends on such factors as scale of operation, cost and availability of raw materials (scraps, highly metallised pellets, etc) and energy (Hans and Rolf, 1988). Today, gas based DRl is more commonly charged to the EAF (Raja, et al, 2005). It offers higher metallisation than coal based and a higher carbon content that can provide chemical energy to EAF operation (Shinjiro, et al, 2003). This usually promotes a "carbon boil" that aids bath reactions.

2.2 Thermal variations and plastic deformation during hot rolling

Hot rolling as a shaping method is the plastic deformation of an engineering material above a temperature at which recrystallisation is spontaneous (Henkel and Pence, 2002). Recrystallisation is a process normally carried out at about 0.6 melting temperature (absolute) of the material involving formation of dislocation-free grains and its growth at the expense of the old deformed grains giving rise to a new structure with low dislocation density. In this temperature range, 850^o-910^oC, the rolling stock structure is substantially free of strain hardening. The hot working process can also be optimized to influence microstructure and properties of the product (Thackray, et al, 2009). This exemplifies the essence of preheating prior sequential plastic deformation. Steady rolling speed is achieved by ensuring that the normal rolling temperature is attained prior the actual rolling leading to reduction in frictional resistance to progressive metal flow through the roll passes (Balogun, 1974).

2.2.1 Preheating

The preheating of the rolling stock is part of the metallurgical requirements of the hot rolling process. Temperature distribution within the roll-stock is the dominant parameter controlling the kinetics of metallurgical transformations and the flow stress (Serajzadeh, et al, 2002). Solution treatment of the roll-stock in the austenitic phase affects the dissolution of solute precipitates resulting from alloying elements such as Mn and Si (Dieter, 1976). Heating also changes the as-cast atomic structure of the constituent components within the roll-stock internal structures. The foregoing is possible only if the stock attained the required rolling temperature and enough time is allowed for complete homogenization of the structure by diffusion. According to Henkel and Pense (1977), the dependence of diffusion on both temperature and soaking time is given by equations 2.2 and 2.3 respectively.

$$D = D_0 \ \exp^{\left(-Q/RT\right)} \qquad 2.2$$

$$X = 1.63(Dt)^{1/2} \qquad 2.3$$

Where D is diffusion coefficient, D_o is a constant having a value of 0.21 cm^2/s for carbon diffusion through austenite, Q is the activation energy, 3380 cal./mol at 900^oC and above, R is gas constant, 1.987 cal./mol.K; X is diffusion depth in cm, T is temperature (K) and t is the time in seconds.

It is evident from equations 2.2 and 2.3 that holding times in the reheating furnace and temperature are important diffusion parameters during reheating of cast materials. Thus, the temperature to which a roll-stock is preheated must be properly controlled in order to avoid the deleterious effect of grain coarsening at high temperature (Alberto, 1995). Today, emphasis is placed more on the synchronization of the continuous caster with down-stream mill processing thereby by-passing the need for reheating prior rolling (Kasuma, et al 1988). This reduces cost of energy and also minimizes weight-loss due to surface oxidation.

The prevalence of high temperature surface reaction on roll-stock necessitates the protection of the reheat furnace atmosphere (Thaller, et al, 2005). Unless protected or measures are taken to prevent such occurrence, reactive elements in the work piece may be embrittled by oxygen. Similarly, uncontrolled furnace atmosphere often results in excessive surface decarburization of the billets. This has been the major source of low yield in many rolling mills. The Technical Bulletin of 1998 reported a loss of up to 5.5kg per billet weight of 109.8kg in a particular rolling mill in Nigeria. This represents five percent weight loss rolled assuming an average of 1140 pieces of billets rolled per shift. At the current price of ₦118, 000 per ton, the loss will be 0.74 million naira per shift of operation. This is considered to be on the high side.

2.2.2 Sequential plastic deformation

Hot rolled product shape is formed by sequential passage of the roll-stock through a series of grooves (Figure 2.3).

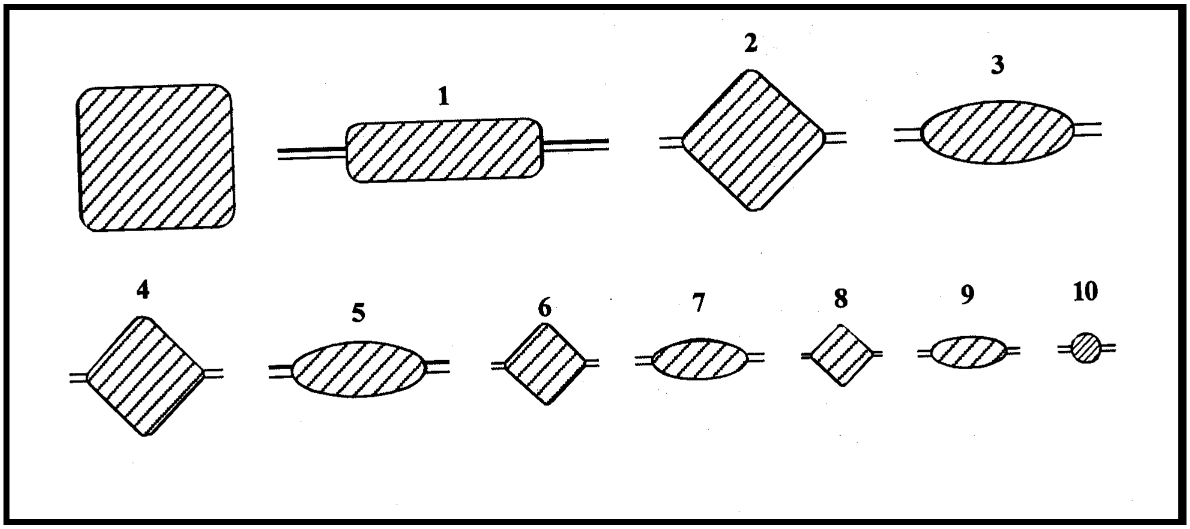

Figure 2.3 Roll-pass sequences for a 100x100 mm cross-section billet reduction to 12mm round bars

Where, 1 is box; 2, 4, 6 and 8 are square-diamond, 3, 5, 7 and 9 are diamond and 10 round passes respectively.

The sequential reduction in the cross sectional area of the roll stock is known as drafting. Drafting schedule influences the final product properties to a large extent due to its influence on recrystallisation and precipitation kinetics. The deformation sequence influences recrystallisation (static and dynamic) phenomenon as it affects the Austenite Grain Size (AGS) of the roll stock and the mechanical properties of the final product. Appropriate roll-pass design is thus a major factor in the success or otherwise of any rolling process (Lundberg,. 1997). According to Wusatowski, (1969) the most frequently used breaking-down sequences are; box pass, diamond pass, square-diamond-pass and square-oval-square. Hence, it is possible to roll a profile from a given bar in an infinite number of ways. The design which accomplishes the rolling of the bar with the fewest number of passes would normally be considered best but may not be the case if roll wear in the individual passes becomes excessive (Appleton and Summad, 2000). Figure 2.4 illustrates the critical stages in the hot rolling process of a conventional mill.

a b c

Figure 2.4 Critical stages in the hot rolling process (a) Reheat furnace (b) Plastic deformation stages and (c) Cooling bed

During hot metal working, strain, strain rate, temperature and microstructure as well as such associated metallurgical phenomena as strain hardening, dynamic recovery and recrystallisation are known to have a significant effect on the flow stress of the metal (Pauskar and Shivpri, 2000). All these phenomena are highly dependent on temperature and rate of deformation (Liu and Lin, 2003). However, the occurrence of dynamic recrystallisation depends on the applied strain, temperature distribution and strain rate field relative to its cross section also impacting significantly on the product properties (Alamu, et al, 2007). It follows from these postulations that the predominant mechanism in hot working is dynamic recovery. This is evident by the occurrence of dislocation substructures in elongated grains (Siamak, 2004).

Dynamic recovery in hot working is the softening mechanism for the work hardening of rolling stock occurring through dislocation climb and cross-slip (McQueen and Ryan, 2002). According to Bergstrom (1983) there exists a fundamental relationship between plastic strain rate and average dislocation velocity. Thus, the extent of plastic deformation a material undergoes is proportional to its dislocation density. However, dislocations in motion often experience resistance in their glide plane requiring the application of certain stress to overcome such resistance. In hot working where dynamic recovery is not possible through dislocation climb and cross-slip, dynamic recrystallisation occurs as the softening mechanism (Pussegona, 1990). These processes occur continuously to varying extents depending on strain, strain rate, temperature, and dwell time throughout the rolling process. Because of hazards and high cost of experimentation, the trend these days is to use mathematical and relevant physical concepts to develop a computer model for the prediction of flow stress and microstructural evolution during hot rolling (Laasraoui and Jonas, 2007).

2.3 Microstructure and mechanical properties of hot rolled steel bar

The mechanical properties of hot rolled steel bars are determined largely by their microstructure as given by grain sizes, texture and volume fractions of the phases present (Barrett and Massalski, 1966). The microstructural evolution that occurs in the roll stock and the final product is dependent on the amount of reduction, strain rate, temperature and extent of holding time between reductions. Influence of extent of deformation has been examined by Kamma and Anagbo (1989) and established that greater than 70 % deformation often result in fine carbide particles. Hurly and Hodgson (2001) through a novel single-pass rolling process achieved ultra-fine (< 2µm) ferrite grains with average austenite grain sizes above 200µm.

It has been long established by Bowering (1968) and Philip and Chapman (1966), that the final properties of hot rolled bars are influenced by the reheating temperature, rate of deformation, temperature of deformation, finishing temperature and the rate of cooling after hot rolling. Of these parameters, the rate of cooling has the greatest influence on the mechanical properties of the bar.

Yen and Liu (1984) and Sangwoo and Peter (2002) have also shown that rolling history greatly influences the microstructure and such mechanical properties as yield stress, tensile stress, strain hardening exponent and elongation of low carbon steels.

There are three feasible microstructures that can be induced in conventional hot rolled steel bar namely pearlite, bainite and martensite depending on the cooling rate (Ming-Chun, et al (2002). These structures often confer varying measure of strength, plasticity, toughness and hardness. Conventional microstructure of hot rolled bars comprises ferrite and pearlite. This structure often confers considerable measure of plasticity with moderate strength and hardness. Zambrano, et al (2001) compared the microstructures of hot rolled bars from both conventional and compact modern mills. Differences in the mechanical behaviours of the bars were ascribed to the differences in their grain size coupled with variations in their textural components.

For mild steel and hypo-eutectoid steels generally, the changes in properties are linear such that they can be related to specific proportions of ferrite and pearlite and their respective volume fractions (Rajan, et al, 1988). Thus, Rudolf and Lehnert (2002) developed a new form of thermo-mechanical treatment of hot rolling known as Hot Rolling in Ferrite Region (HRF). By this technology, it is possible to produce hot rolled bars with enhanced quality parameters. However, such rolled products are usually dedicated for special applications.

It was established (Sameer, et al, 2004, Choi and Kertesz, 2002) that martensitic structure on the surface with a stratified mixture of ferrite and pearlite in the core is the type of microstructure that confers markedly improved mechanical properties of steel bars. Only the lower bainitic structure exhibits comparable strength to the dual structure. However, drastic critical cooling rate is required to quench mild steel to martensite (Honeycombe and Bhadeshia, 1996). After hot rolling, the challenge is to establish such a critical cooling rate that induces in the rolled bar either martensitic or bainitic microstructure.

Control of temperature during cooling is essential for achieving desired mechanical and metallurgical properties (Saroj, et al, 2004). This is predicated on the effect of austenitising temperature on the microstructure and mechanical properties of hot rolled steels (Jones, et al, 2006). In the works of Lai, et al (2007), transmission electron microscopy revealed an apparent large increase in the amount of retained austenite in the specimens austenitised at higher temperature. Austenitising at 870°C resulted in virtually no retained austenite and its yield strength improved correspondingly. Helmult (1992), Harry and Rainer (1996) and Respen and Mario (2001) obtained similar results in their attempt to devise methods for temperature control during hot rolling.

The implication of these results for steel microstructure is that, grain structures of varying sizes and morphology can be developed through a logical simulation of relevant metallurgical parameters. This is to be expected as cooling rate in association with the chemical composition govern the nucleation and growth behaviour of austenite to ferrite phase transformation during cooling (Elmer, et al, 1989). The carbon content influences both the propensity to martensitic transformation and the morphology of the carbide that forms during cooling (Akiyama, et al, 2002). Consequently, the grain morphology obtained depends on the cooling rate and the solidification process validating the profound influence of cooling rate on the microstructure of steels (Yada, 1987).

Apart from temperature, the mechanical properties of hot rolled steel are determined both by the structure developed through a given cooling pattern (Salvador, 2001). Commercial cooling media include air, water, molten salt and combination of either of these media. Air-cooling appears to be prevalent in conventional rolling mill. Beside the conventional air-cooling approach, a host of other innovative cooling methods have been developed to meet the ever-increasing demand for rolled products with superior strength characteristics. These include among others, grain refinement by control of recrystallisation (Cuddy, 1984), controlled rolling and Ferrite-Pearlite transformation (Inagaki, 1986) and Ferrite grain growth and transformation mechanism (Houbaert, et al. 2005).

The main principle employed in modern rolled product strength optimization entails the use of a cooling regime that achieves desired metallurgical properties. Such principle is employed in the following processes; in-line accelerated cooling, quenching and in-line annealing. Recently, Temperature Controlled Rolling (TCR) process was developed (Mukhopadway and Sikdar, 2005). It entails the arrangement of cooling lines throughout the mill with optimized distances between the stands for cooling and equalization. This allows for a guaranteed programmable finished product quality.

2.4 Hot rolled steel bars mechanical properties enhancement techniques

There are two main metallurgical methods of optimizing mechanical properties of hot-rolled steel bars namely; addition of alloying elements such as Cr, Mo, W, V, etc and process control (Mudiare, 1977). The alloying addition method can only be effective if employed with process control while the latter can be used independently with good results (Lotter, 1991). For reason of cost, alloying addition technique is rarely employed in the production of commercial carbon steel profiles for construction purposes. The present study will therefore not dwell further on the method.

2.4.1 Process Control (PC)

According to Ryoichi (2001), process control is one of the recent innovations aimed at improving strength. The technique encompasses two distinctive but complementary processes namely Controlled Rolling (CR) and Controlled Cooling (CC). Controlled Rolling (Ryoichi, 2001) is a means of improving the strength and toughness of steel bar through the optimization of hot rolling conditions such as reheating furnace environment, roll-stock composition and finishing temperature at the last stand. Augusti (1998) employed the combination of controlled rolling temperature and stresses generated during rolling to evolve microstructures that optimised mechanical properties. In contrast to CR, controlled cooling is a variation of Thermo-Mechanical Treatment (TMT). Thermo-mechanical strengthening technique involves varying solution treatments that include grain-size refinement, strain hardening, solid solution strengthening and precipitation hardening. All these phenomena create substantial impediments to the motion of dislocation which give rise to improved strength characteristics (Bai, et al, 2003).
The approach is to develop the desired microstructure by controlling the temperature of the hot rolled stock as to transform it from the austenite phase to different volume fractions of martensite, pearlite and ferrite phases (Sameer, et al 2004).

Ray, et al (1997) carried out a practical comparison of the strength developed through thermo-mechanical treatment (TMT) of plain carbon steel and copper bearing alloys. The quenching parameters were altered to achieve different yield strength levels. Both the plain carbon and alloyed steel grade TMT bars exhibited a composite microstructure consisting of ferrite-pearlite at the core and tempered martensite at the surface. The bars also conformed to strength requirements in the range of 500-550 MPa with good elongation values (21-28%) and excellent bendability. This showed that plain carbon steel could be treated to develop strengths comparable to those of alloy steel grades.

Solid solution hardening principle was employed in the development of Tempcore and Thermex processes. Both processes were developed and patented in the mid-eighties to meet the challenge of low strength characteristics prevalent with conventional hot rolled mild steel bars (Markan, 2004). The processes employ the principle of martensitic transformation through drastic cooling of hot rolled steel bars immediately after the finishing stand. However, industrial isothermal transformation of austenite to martensite in mild steel requires a critical cooling rate up to 500 ^{0}C/s and must be accomplished within five seconds at most (Saroj, et al, 2004). This is often difficult to achieve. Thus, Tempcore and Thermex processes are fraught with two major constraints that have made their adoption difficult. One is the high cost of re-engineering of a typical conventional mill for Tempcore or Thermex process technology. The other is the lack of information on process operating variables because of patent restrictions. Presently, three grades of reinforcing steels are available for the construction industry in Europe (Nikolaou and Papadimitriou, 2004). The steels are those produced by Tempcore process, microalloying with vanadium and work hardening.

2.4.2 Development of an alternative microstructure

Dotreppe (2006) established that without innovative hot rolling, steel bars produced through conventional route cannot exhibit adequate yield strength. One of the efficient and cost effective means of achieving improvement on the mechanical properties of conventional hot rolled steel bars may therefore, be found in developing an alternative microstructure in which the grains and texture are different from pearlite developed in conventional rolling.

Grain structure (size, shape and texture) is one of the primary characteristics that determine the mechanical properties of metals and their alloys (Henkel and Pense, 2002). This is predicated on the relationship that exists between grain-size and grain boundary on one hand and the interference of the latter with dislocation motion on the other (Curtin and Dewald, 2005). The interactions of dislocation with each other by slip and with surrounding crystal microstructures through cross-slip, glide and climb often result in enhanced strength in metals.

Grain structures of varying sizes and morphology can be developed through a logical simulation of varying degrees of under cooling of steel bar from the austenitising temperature (Yada, 1987).

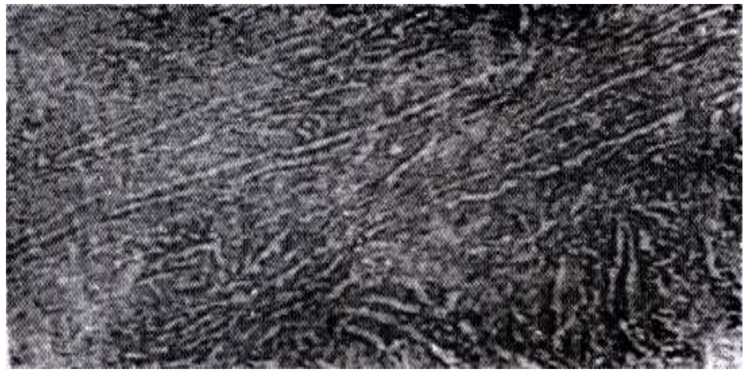

Plate 2.1 Pearlite microstructure (Vijendra, 2004)

The predominant microstructure of steel bars produced in conventional mill is pearlite, which comprises ferrite and cementite (see Plate 2.1).

The ratio of ferrite to cementite in pearlite is 7:1 which accounts for the steel's characteristic considerable measure of plasticity, low strength and marginal hardness (Oelmann and Davies, 1983). Zambrano, et al (2001) compared the microstructures of hot rolled bars from conventional and compact modern mills. Bars from the compact mill exhibited a dual-phase structure (see Plate 2.2) of martensite-pearlite. Differences in the mechanical behaviours of the bars were ascribed to the differences in their grain size coupled with variations in their textural components (Samuel, 1990).

a b

Plate 2.2 Martensite morphology (a) Lath and (b) Plate (Raghavan, 2006)

The formation of martensite however, requires drastic cooling rate, which is practically difficult to achieve in mild steel. Alternatively, a well controlled fast cooling of austenite could be effected such that lower bainitic microstructure is formed. This can be achieved through what can be described as a middle course critical cooling rate, which is between drastic quenching as obtained in martensitic hardening and air-cooling as obtained in conventional rolling. Development of bainitic structure in steel by this method will constitute a significant improvement on the conventional pearlitic structure. This is because lower bainite microstructure is known to confer enhanced strength property on the bar (Kumar, et al, 2008).

2.4.3 Synopsis of bainitic transformation

Bainite is a generic term used to describe one of the products of austenite decomposition either in isothermal or continuous cooling (Figure 2.5). Bainite morphology and classification depend on mode of transformation (Bramfitt and Speer, 1990). The work of Edmonds and Cochrane, (1990) showed that bainitic microstructure can be produced in a variety of steels either as a deliberate attempt to achieve a particular combination of strength and toughness or in response to welding during fabrication.

Generally, bainite is an aggregate of ferrite and carbide. Based on composition and transformation temperature (Ohtani, et al, 2007) three types of carbide are possible namely, cementite, Є-carbide (Fe_xC) and normal carbide (FeC).

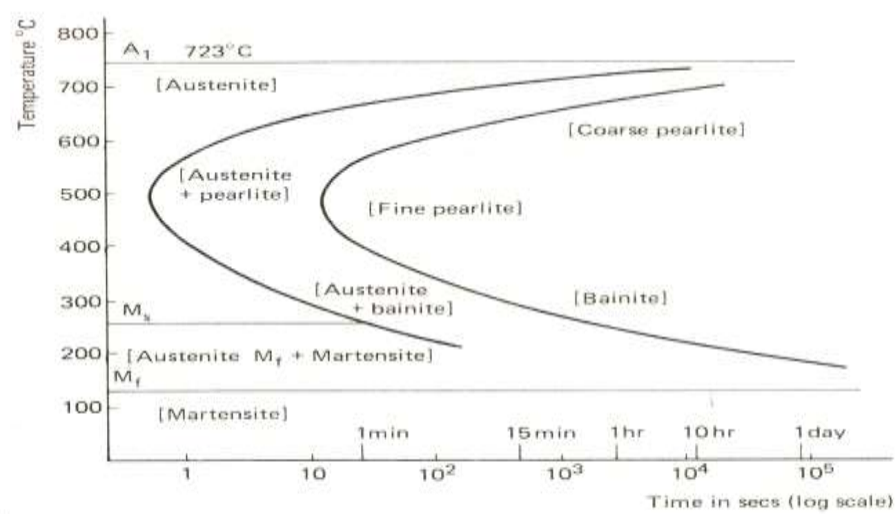

Figure 2.5 Time-Temperature Transformation Curves for Eutectoid Steel

(Oelmann and Davies, 1983)

It has been established (Yusuya, 2007) that bainitic reactions are feasible in all grades of carbon steels. However, inducement of bainitic structure is not easily achieved experimentally due to the overbearing influence of pearlite and martensite transformation (Raghavan, 2006). The partition of carbon between these phases, precipitation of cementite and other carbides and relaxation strain are also responsible for the complexity of the bainitic transformation (Honeycombe and Pickering 1972). Addition of small amount of alloy elements such as boron, chromium and molybdenum are often employed to obtain full bainitic steel. This approach is not popular because of high cost except in steels for special application such as pressure vessels, pipes for gas and oil, aircraft structural components, e.t.c.

Bainitic transformation of austenite is initiated when on fast undercooling the ferrite formed grows by rejecting excess carbon to the surrounding regions in the matrix where carbide eventually nucleates (Vijendra, 2004). This implies that the transformation of austenite to bainite requires the diffusion of carbon to proceed (Figure 2.6).
However, the nucleation and growth rate of ferrite decreases with increasing carbon content (Yasuya, 2007). Bainitic microstructure is divided into upper and lower categories based on morphology and temperature of transformation.

Upper bainite forms in the temperature range of 550^{o}-400^{o}C and exhibits feathery-shaped ferrite. The feathery appearance arises from clusters of ferrite laths between which cementite platelets have precipitated in a direction parallel to the length of the laths. Based on texture, upper bainite exhibits mechanical characteristics similar to those of pearlite.

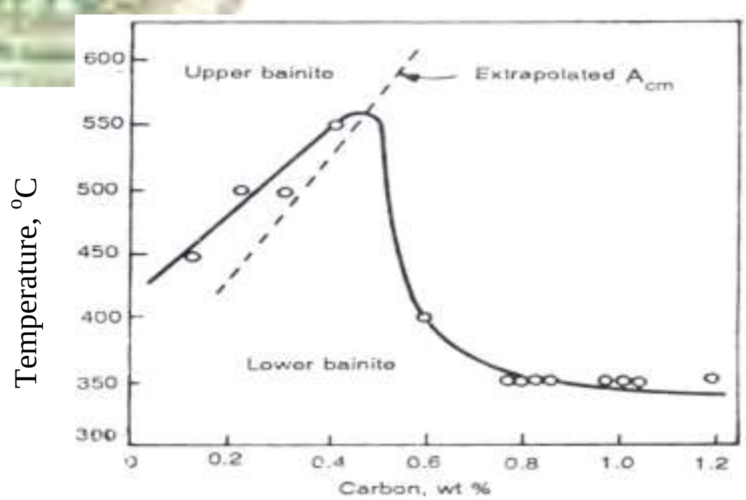

Figure 2.6 Effect of Carbon on the Temperature for Change from Upper-Lower Bainite (Vijendra, 2004)

Lower bainitic structure (Plate 2.3) forms in the temperature range of 250^0-400^0C by a shear transformation of austenite at cooling rates faster than air-cooling. The structure consists of ferrite solid solution saturated with carbon and particles of carbide occurring isothermally or athermally (Rollason, 1973).

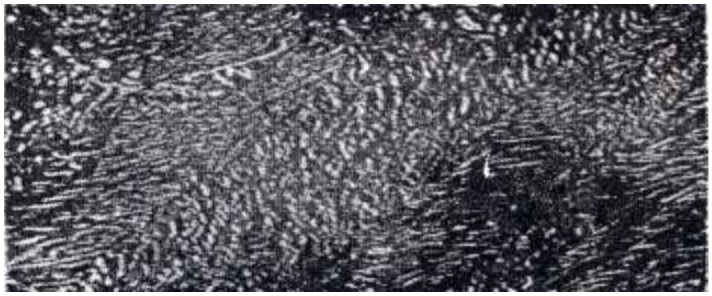

Plate 2.3 Lower bainite microstructure (Vijendra, 2004)

The thermal treatments represent industrial conditions involving such cooling rates too fast for austenite to form pearlite but not rapid enough to produce full martensite. Unlike in pearlite, the carbide particles in lower bainite are located within the plates of the α-phase due to the sluggish diffusion of carbon. This results in high dislocation densities in the bainite microstructure. Most polycrystalline materials contain dislocation density in the range 10^8 - $10^{12}cm^{-2}$ (Dieter, 1976) while that of lower bainite is in the range of 10^{15}-$10^{16}cm^{-2}$ (Vijendra, 2004). The carbide particles dispersed within the ferrite phase field act as barrier to the motion of dislocation, which enhances the bar's strength considerably (Schaffer et al, 1999).

Bainitic steel is one of array of engineered materials in high demand in the construction industry. The application of bainitic transformation (BT) is extensively used in the industry to strengthen critical structures and machine components. Lower bainitic steels (LBS) also, have widespread applications in structural members of bridges, cranes and other structures (Arvedi and Guindani, 2004). The high strength properties of LBS (Figure 2.7) are due to the interstitial atoms of carbon and the high dislocation density in the α-martensitic phase (Henkel and Pence, 2002). Similarly, the formation of inclusion of dispersed carbides in the α- solid solution is also responsible for high hardness, strength and ductility of LBS.

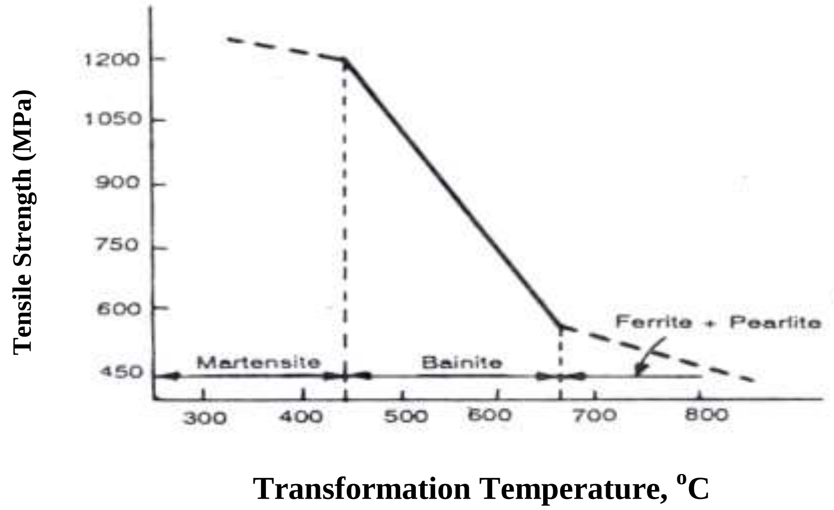

Figure 2.7 Influence of transformation Temperature on Tensile Behaviours of Plain Carbon Steel (Vijendra, 2004)

Prospects of achieving substantial austenite transformation into lower bainite in mild steel highly recommend the BT over the martensitic transformation (MT). This is because solution transformation in mild steel if not effectively carried out often results in retained austenite, which is a precursor for ageing. Development of bainitic structure in mild steel through spray quenching is also favoured for reason of lower cost. Other heat treatment processes that may give rise to bainitic structure include austempering and marquenching (Yu, 1983). However, more expensive equipment is required to accomplish either of the two processes, which need a quench holding bath between 400^0C and 250^0C before subsequent cooling to a lath/plate martensitic structure. In a bid to overcome some of the foregoing constraints and challenges, attempt has been made in this study to develop a new microstructure, lower bainite, in hot rolled mild steel bar through spray-quenching (SQ) on the cooling bed. Lower bainite microstructure is completely different from pearlite, which is the predominant phase in conventional steel bar.

CHAPTER THREE

3.0 METHODOLOGY

3.1 Conceptual framework

The concept of solid solution hardening was employed in the design of the experimental procedures in this work. Solid solution hardening is an effective metallurgical technique for strength characteristics improvement in metals and alloys (Rollason, 1973). The mechanism entails inducement of non-equilibrium phase transformation that results in asymmetric lattice distortion. Distorted lattice has been found to offer resistance to dislocation movement prevalent with interstitial elements such as carbon in steel thereby leading to improved strength characteristics (Dieter, 1976). The knowledge of the mechanism by which the phenomenon occurs provides practical method to achieve desired structural transformation in the rolled product.

During heat treatment, hypo-eutectoid steels are normally heated to the upper critical point, 910^{o}C to ensure the formation of stable austenite (Krauss, 1984). This temperature corresponds to the upper range of finishing temperatures for the hot rolling process (Jeff, et al, 2007). The type of structure induced in the rolled steel however depends largely on the cooling rate. Consequently, effective solution to the problem of low strength characteristics of conventional hot rolled steel bar sum-up into two viz:

(i) Establishment of appropriate finishing temperature for the conventional rolling operation. This is the point at which transformation starts.

(ii) Establishment of appropriate cooling rate. This is the energy that drives the transformation. Cooling rate also influences microstructural integrity of the rolled bar in terms of grain size, shape and texture.

The above tasks were executed through a new process tagged "Temperature Tracking- Jet Water Spray" (TT-JEWAS). The process is an innovation of the thermo-mechanical treatment of hot rolled steel bar. It is highly flexible and cost effective. TT-JEWAS process employs a two-pronged approach namely temperature tracking and heat treatment-spray quenching.

3.2 TEMPERATURE TRACKING EXPERIMENT (Industrial Scale)

This is aimed at obtaining the hot rolling thermal variations at critical stages of the operation and the corresponding mechanical properties of the rolled product. The objective is to establish the appropriate finishing temperature range for the process. These two approaches taken together portray the metallurgical and technological dynamics of the entire rolling process.

3.2.1 Material

The material used is cast steel billets, 100mm x 100mm x 1600mm (Figure 3.1) and the chemical composition obtained through optical emission spectroscopy is shown in Table 3.1. Prior to rolling, the billets were charged into re-heat furnace and heated to rolling temperatures in the range 1000^{o}–$1200^{o}C$ from which several pieces of 12mm diameter high-yield reinforcing bars were rolled. One hundred and twenty billets (maximum capacity of reheat furnace) were rolled in each of the seven rolling batches monitored. It took between 90 and 105 seconds to complete the rolling of a billet. This culminated into different finishing temperatures for each rolling batch.

Table 3.1 Chemical composition analyses of rolling stocks (billets)

Rolling Batch	ELEMENTS (%)												
	C	Si	S	P	Mn	Ni	Cr	Sn	Mo	V	Cu	Fe	* Ceq
1	0.194	0.167	0.039	0.025	0.856	0.146	0.178	0.038	0.029	0.006	0.344	97.978	0.42
2	0.220	0.199	0.046	0.032	0.501	0.101	0.104	0.036	0.015	0.003	0.216	98.454	0.35
3	0.164	0.123	0.046	0.027	0.768	0.137	0.149	0.037	0.017	0.002	0.318	98.336	0.36
4	0.308	0.258	0.050	0.028	0.684	0.117	0.147	0.037	0.015	0.002	0.342	98.012	0.49
5	0.211	0.246	0.039	0.028	0.506	0.112	0.148	0.035	0.013	0.002	0.306	98.354	0.36
6	0.172	0.113	0.046	0.019	0.697	0.105	0.136	0.035	0.019	0.001	0.249	98.686	0.34
7	0.231	0.250	0.055	0.034	0.602	0.102	0.120	0.034	0.020	0.002	0.274	98.276	0.38

*Ceq is the chemical equivalent value determined by equation 2.1.

$$Ceq(\%) = C + \frac{Mn}{6} + \frac{Cr + Mo + V}{5} + \frac{Ni + Cu}{15}$$ **(See page 13)**

Figure 3.1 Cast steel billets (rolling stock)

3.2.2 Temperature Tracking (TT)

Using a Jenway digital pyrometer model 220k, monitoring of the process temperature was carried out at each of the critical points where high temperature deformation occurred namely roughing, intermediate and finishing stands respectively. As illustrated in Figure 3.2, temperature was measured at the exit of reheat furnace, on the rolling stock in-between the roughing, intermediate and finishing stands respectively.

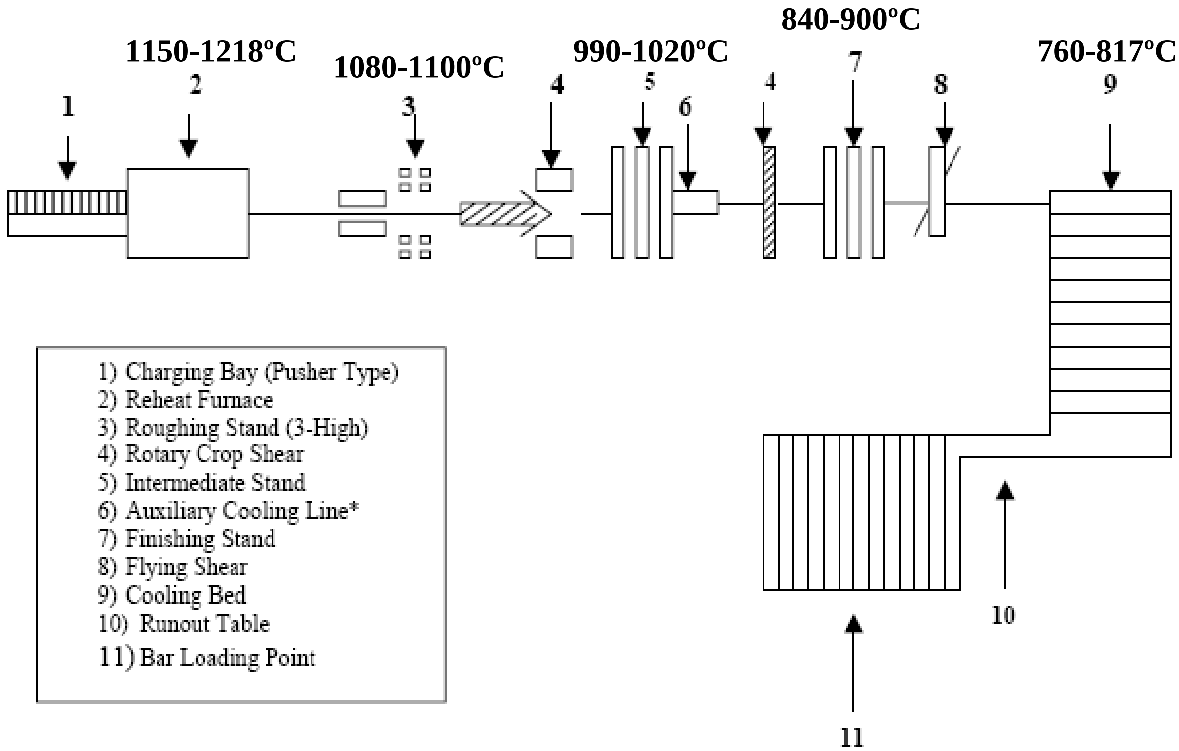

Figure 3.2 A Conventional Bar Mill Configuration

Further, the product temperature before cooling was measured at the cooling bed. The cooling bed is a platform on which rolled bars are allowed to air- cool for some minutes prior to bar sizing and bundling. Bar samples of 12mm were obtained at the end of each rolling batch for mechanical testing and microstructural analyses.

3.2.3 Mechanical property tests

A specimen each from the rolling cycles was obtained and identified as A, B, C, D, E, F, and G for tensile test. In carrying out mechanical property evaluation, test specimens were prepared according to the British standard (BS EN 10002-1). Relevant clauses of the Nigerian Industrial Standards (NIS 117-42/50HD 2004) were also complied with. The test specimens hardness values were evaluated using the 'B' scale Rockwell hardness machine model United TB-II. An Instron electro-mechanical testing system model 3369 was used to obtain the yield and tensile strengths of the specimens. A typical shape of the tensile test specimen is shown in Figure 3.3

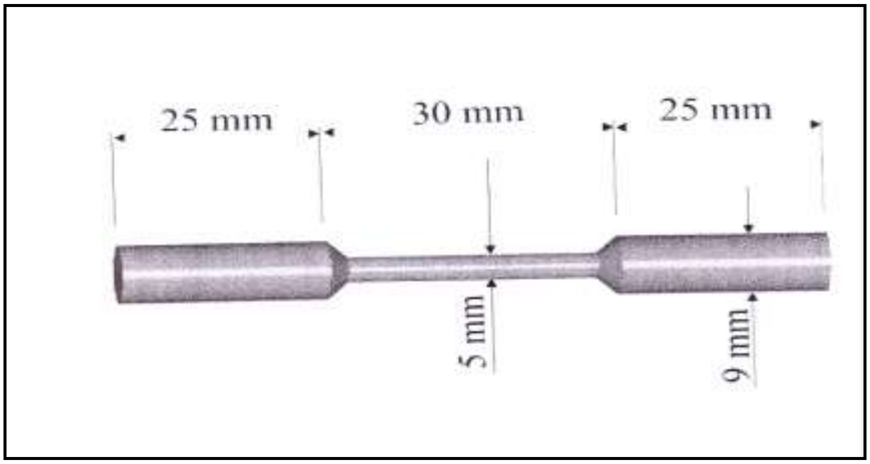

Figure 3.3 Standard Tensile test specimen

3.2.4 Microstructural analysis

Test specimens were ground on a water-lubricated grinding machine using silicon carbide abrasive papers grades 240, 320, 400 and 600 grits. Final polishing of the specimens was effected with 0.5µm chromic oxide powders. The surfaces so obtained were etched in 2% Nital solution for 30 seconds and rinsed in water. The microstructural features of the specimens were examined under a metallurgical microscope model FEROX PL at x 800 magnification.

3.3 HEAT TREATMENT AND SPRAY QUENCHING EXPERIMENT (Laboratory Scale)

This experiment is meant to replicate in the steel the finishing temperature earlier established during the temperature tracking experiment and to simulate varying cooling rates that are substantially faster than the conventional air-cooling. The objective is to induce in the steel a new microstructure that confers markedly improved strength characteristics.

3.3.1 Material and Specimen Preparations

Hot rolled steel bar, NST 42/50HD (AISI 1030, BS 970) was obtained from the stock of the 12mm steel bars shown in Figure 3.4 and the chemical composition including its carbon equivalent value (**Ceq)** is presented in Table 3.2.

Table 3.2 Chemical composition of material used for Heat Treatment and Spray Quenching

ELEMENTS (%)	

C	Si	S	P	Mn	Ni	Cr	Sn	Mo	V	Cu	Fe	Ceq
0.231	0.250	0.055	0.034	0.602	0.102	0.120	0.034	0.020	0.002	0.274	98.276	0.38

Figure 3.4 High yield hot rolled steel bars (12mm)

From the sample, forty-nine (49) specimens were prepared for both hardness and tensile tests according to the British standard EN-10002-1 (formerly BS 18) and the Nigerian Industrial Standards (NIS 117-42/50HD 2004). These tests were meant to evaluate after necessary treatments and under static loading the steel's strength, ductility and wear/abrasion resistance.

3.3.2 Heat treatment of specimens

Test specimens were heated at the rate of 10^0C/min in a muffle furnace (Figure 3.5). The specimens were divided into seven groups identified as **A_1-A_7, B_1-B_7, C_1-C_7, D_1-D_7, E_1-E_7, F_1-F_7** and **G_1-G_7** representing respectively the austenitising temperatures of 800^0, 820^0, 840^0, 860^0, 880^0, 900^0 and 1000^0C.This temperature range falls within the intercritical ($\alpha + \gamma$) region of Fe-C equilibrium diagram on one hand and a simulation of typical hot rolling finishing temperatures on the other. The adoption of the temperature range is aimed at eliminating the conventional α -pearlite structure in the steel bar and replacing it with α-austenite to facilitate efficient transformation on fast cooling. The specimens were soaked for between 20 and 30 minutes for homogenization.

Figure 3.5 Muffle furnace

Figure 3.6 0.5HP water pump

3.3.3 Spray quenching of heat-treated specimens

According to industrial standard practice, 10,000litres/ton of water at ambient temperature is required to quench-harden plain carbon steel. This translates to 10litres/kg or 10ml/g water requirements. Given that each test specimen weighs 32.1g, approximately 0.321litres of water at ambient temperature is required to quench harden a test specimen. Therefore, a typical 12 mm commercial steel bar weighing 10.658 kg will require 106.6litres to quench harden it. Similarly, at an average production rate of 200 tons/day, about two million litres of water will be needed at the cooling bed. This volume of water is massive in view of the logistics that will be involved in its delivery and maintenance. In this study, attempt was made to reduce the volume of water requirement by adopting pressurized spray quenching. Spray quenching under pressure enhances fast cooling as the formation of passive blanket film around specimen is prevented (Sikdar and John, 2007). Thus, 200ml of water was used in each spray-quench cycle of test specimens. This represents 37.7% reduction in water requirement daily.

Spray quenching of specimens was carried out using a medium capacity, **0.5HP (0.37KW)** water pump (Figure 3.6). With appropriate variations in the piping-in and out of the pump, water flow rates **(ml/s)** of 40, 20, 13.3, 10, 8, 6.7 and 5 were achieved. At the end of each cooling cycle, a digital pyrometer was used to measure the temperature of test specimens. Figure 3.7 shows the experimental set-up for the spray-quenching of heat treated specimens.

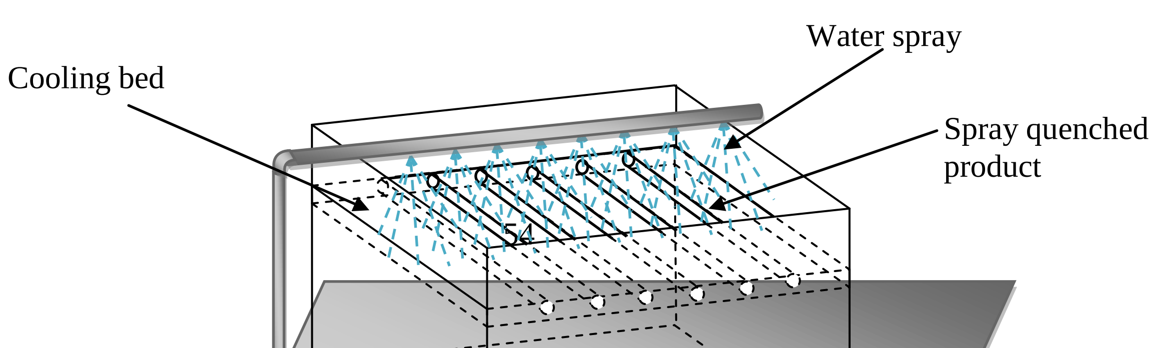

Figure 3.7 Set-up of water spray-quenching experiment

3.3.4 Mechanical tests and Microstructural Analysis

An Instron electro-mechanical tester model 3369 (Figure 3.8) operated at a crosshead speed of 10mm/min. was used for the tensile tests. Specimen hardness values were evaluated using the Rockwell 'B' scale. The specimens, which were seven in each group, were identified as **A_1-A_7, B_1-B_7, C_1-C_7, D_1-D_7, E_1-E_7, F_1-F_7** and **G_1-G_7**.

Instron electro-mechanical Tester

Avery Impact Tester

Rockwell Hardness

Figure 3.8 Mechanical properties testing equipment

Application of structural steel bars under dynamic loading such as in bridges and buildings constructed along seismic prone areas are commonplace. Therefore, hence, evaluation of the bar's susceptibility to brittle fracture under such conditions is imperative. Consequently, another forty nine square charpy -v impact energy test specimens (Figure 3.9) of 10x10mm cross-section and 50mm long with a notch 2mm deep at the middle of one of the sides and an included angle of 45^0 were prepared in accordance with BS 131 (Parts 1-5). The specimens were then subjected to impact loading using Avery impact tester (type 6703) at ambient temperature and a striking pendulum velocity of 5m/s. Energy absorbed at failure by each of the test specimens was read off from the scale.

Figure 3.9: Fractured Charpy-v Impact Test specimens

Figure 3.10: Specimen polisher and Resin caster

Another forty-nine (49) specimens were prepared by grinding on a water-lubricated grinding machine (Figure 3.10) using varying grits of silicon carbide abrasive papers. The microstructural features of the specimens were examined under metallurgical microscope model FEROX PL at x 800 magnification.

CHAPTER FOUR

4.0 RESULTS AND DISCUSSION

4.1 Finishing temperatures of conventional rolling process

Results of the temperature tracking experiment are shown in Table 4.1.

Table 4.1 Temperature Tracking Data (TTD)

Rolling	Reheat	Temperature at the stands (^{0}C)	Cooling

Batch	furnace T_o (^{0}C)	Roughing T_r	Intermediate T_i	Finishing T_f	bed T_c (^{0}C)
1	1217	1085	1013	872	792
2	1215	1075	998	848	762
3	1218	1094	1026	893	817
4	1209	1074	1005	864	786
5	1215	1078	1003	858	774
6	1216	1087	1016	879	800
7	1214	1076	1000	853	768

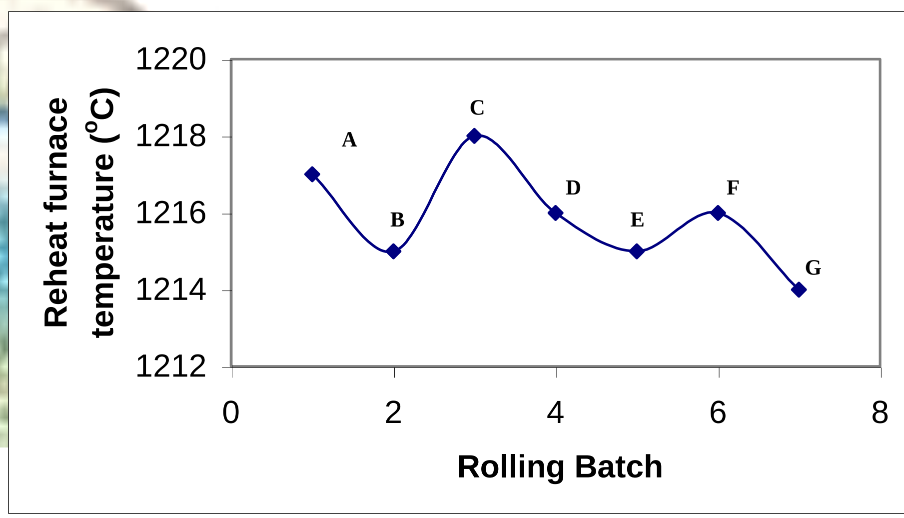

Figure 4.1 Variation of reheating temperature of billet with rolling cycle

Figure 4.1 shows the variation of reheat temperatures, T_0 of billets used during the rolling cycles. The values were almost the same, 1216± 2^0 C. The finishing temperatures, T_f however, vary widely and in the range 848.2-893.4 ^{0}C.This gives a variation of 45.2 ^{0}C, which is high enough to induce microstructural transformations during the air- cooling of the bars. Wide variations in finishing temperatures can be attributed to the combination of two factors namely, in-process cooling and speed of rolling. This is exemplified by the amount of frictional force required to accomplish the desired deformation at each roll-pass. The combination of direct and indirect cooling of rolling stock along with other heat sensitive devices of the mill facility impact on the finishing temperature. Other than technology, internal state of the rolling stock (Pereloma, et al, 2001), in terms of cleanness, affects the extent of strain hardening suffered during rolling hence, the speed of rolling. Similarly, large amount of strain hardening occasioned by inclusions usually give rise to delay in material flow (Mauder and Charles, 2006).

4.1.1 Microstructural Observation of air-cooled steel

The microstructural features of test specimens are shown on Plate 4.1 (A-G).

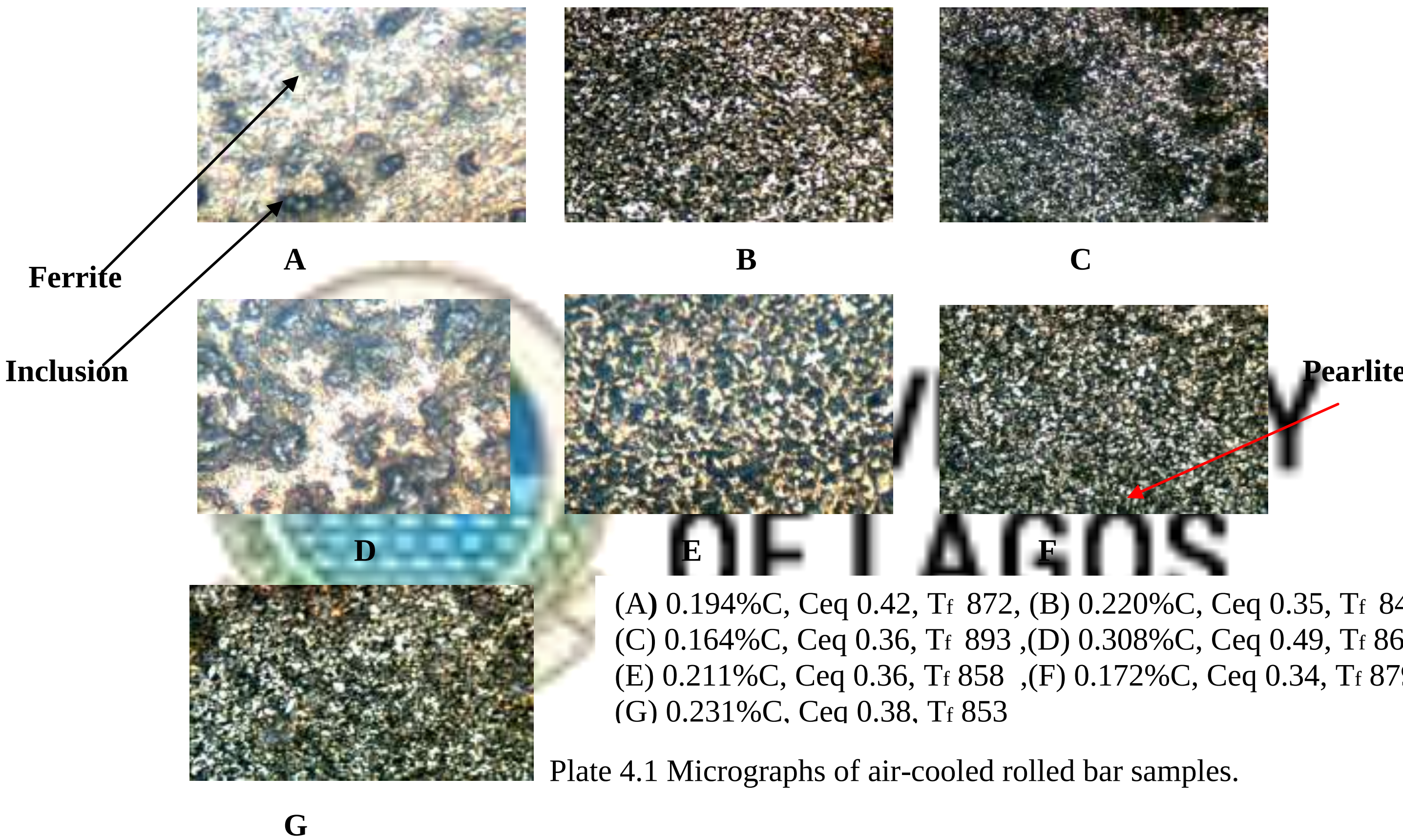

(A) 0.194%C, Ceq 0.42, T_f 872, (B) 0.220%C, Ceq 0.35, T_f 848
(C) 0.164%C, Ceq 0.36, T_f 893 ,(D) 0.308%C, Ceq 0.49, T_f 864
(E) 0.211%C, Ceq 0.36, T_f 858 ,(F) 0.172%C, Ceq 0.34, T_f 879
(G) 0.231%C, Ceq 0.38, T_f 853

Plate 4.1 Micrographs of air-cooled rolled bar samples.

The micrographs A-G show two major phases, ferrite and pearlite including large pod-like non-metallic inclusions. The volume fractions of the phases are as presented in Table 4.2. V_{vp}, V_{vf} and V_{vi} are the volume fractions of pearlite, ferrite and inclusions respectively.

Table 4.2 Volume Fraction Analyses of Constituent Phases

	Volume Fractions (V_v)		
Specimen Micrograph ID	$\frac{Pearlite}{V_{vp}}$	$\frac{Ferrite}{V_{vf}}$	$\frac{Inclusions}{V_{vi}}$
A	0.61	0.24	0.15

B	0.77	0.11	0.12
C	0.65	0.22	0.13
D	0.64	0.19	0.17
E	0.66	0.21	0.13
F	0.62	0.26	0.12
G	0.71	0.15	0.14

One of the fundamental quantitative stereological measurements in microstructure of steel bars used for reinforcement purposes is the volume fraction, V_v of the constituent phases. Quantitative stereology is a body of methods for the exploration of three-dimensional space when only two-dimensional sections through solid bodies or their projections on a surface are available (De Hoff, 1968). The techniques provide for the means by which informed conclusions on the volumetric characteristics of the specimens' microstructure are based (George and Vander, 2007). In this study, volume fractions of each constituent phase were estimated in proportion to the areas occupied in the matrix. From Plate 4.1 the predominant phases are pearlite and ferrite. Generally, fine-grained pearlite and $V_v \geq 70\%$ confers a relatively high strength on the steel whereas ferrite imparts ductility (Oelmann and Davis, 1983). Strength and ductility exhibited by the specimens are dependent on the volume fractions of the phrases in the steel.

The rolling cycles monitored in this study had their finishing temperatures between 864^0 and 893.4^0C indicating about 150 ^{0}C above the lower critical point, 721^0C. Hence, some 14 seconds elapsed before the start of transformation. The delay resulted in the formation of coarse pearlite in test specimens at finishing temperatures of 872^0, 893^0 and 879^0C respectively (see Plate 4.1: A, C, F). However, the degree of coarseness of the pearlite reduces with decreasing finishing temperatures (see Plate 4.1 (E) T_f 858^o, (G) T_f 853^o and (B) T_f 848^o C). Coarse pearlite formed at the nose of TTT curve just below A_1 line exhibits high strength but poor ductility (Oelmann and Davis, 1983). This accounts for the low yield stress exhibited by all test specimens except specimen G (452.8MPa) as shown in Figures 4.3 and 4.4.

4.1.2 Ultimate Tensile Strength of air-cooled bar

Using the data obtained during tensile test on specimens (Appendix A, Tables A1-A3), relevant tensile data are computed and presented in Table 4.3. Appendix B contains the Matlab programme for the stress-strain behaviours of the air-cooled steel specimens. The effects of microstructures in conjunction with other relevant parameters such as temperature, composition and cooling regime manifested in the flow curves of Figure 4.2.

Table 4.3 True stress-strain data of conventional hot-rolled steel

A: Ro=23.14, a=19.46mm^2		B: Ro=23.53, a=20.11mm^2		C: Ro=23.36, a=19.32mm^2		D: Ro=26.21, a=20.67mm^2		E: Ro=23.37, a=20.19mm^2		F: Ro=24.92, a=21.73mm^2		G: Ro=22.38, a=19.71mm^2	
True **Stress (MPa)**	True Strain ε	True Stress (MPa)	True Strain E	True Stress (MPa)	True Strain ε	True Stress (MPa)	True Strain ε	True Stress (MPa)	True Strain E	True Stress (MPa)	True Strain ε	True Stress (MPa)	True Strain ε
210.7	0.02	256.6	0.03	56.0	0.01	179.8	0.02	101.0	0.01	99.0	0.01	157.4	0.01
266.8	0.03	336.1	0.04	107.2	0.01	225.8	0.03	153.1	0.02	189.2	0.02	260.8	0.02
321.8	0.04	366.6	0.05	158.9	0.02	296.4	0.04	256.1	0.03	285.3	0.03	315.1	0.03
379.4	0.05	444.9	0.06	215.3	0.02	354.1	0.05	339.5	0.04	336.0	0.04	367.4	0.03

448.1	0.09	488.3	0.09	267.1	0.03	435.9	0.06	417.6	0.05	414.7	0.08	442.2	0.04
518.0	0.11	585.0	0.12	323.5	0.04	500.5	0.07	482.1	0.09	498.4	0.11	499.2	0.05
535.4	0.12	634.5	0.15	396.1	0.06	559.8	0.10	586.0	0.12	553.6	0.15	553.6	0.09
586.8	0.16	652.2	0.16	507.1	0.12	672.9	0.12	651.3	0.16	591.5	0.18	648.4	0.12
614.3	0.19	692.6	0.19	604.6	0.22	748.8	0.16	696.1	0.20	623.0	0.22	749.6	0.20
618.8	0.20	712.1	0.22	616.7	0.25	801.5	0.20	711.4	0.23	635.5	0.25	773.2	0.24
596.4	0.23	728.2	0.25	588.3	0.28	806.9	0.21	680.6	0.26	645.7	0.28	745.8	0.27
531.5	0.25	607.5	0.30	480.1	0.30	676.2	0.27	563.3	0.29	484.9	0.35	624.6	0.30
298.0	0.25	361.8	0.30	268.9	0.31	381.9	0.28	328.1	0.29	290.8	0.35	344.5	0.30
E (MPa) 16551.4		16117.0		17347.1		13493.6		16892.5		17612.0		19157.9	

Note:

Ro-original gauge length, a-cross sectional area of specimens A, B, C, D, E, F and G respectively, E-Young's modulus of each specimen measured during tensile test

Specimen D exhibited the highest ultimate tensile strength, 806.9MPa mainly due to its relatively high carbon concentration (0.30 per cent) coupled with high concentrations of inclusions (Ceq 0.49), which coalesced along with pearlite grains. This type of structure impedes dislocation mobility thereby requiring higher stress to cause plastic deformation. However, the bar is not recommended for use as reinforcement because of its abysmally low modulus of elasticity, 13493.6MPa (Table 4.3). Similarly, specimens A, C and F exhibited relatively low ultimate tensile strengths 618, 616 and 645 MPa respectively due to coarse pearlite formed at higher finishing temperatures.

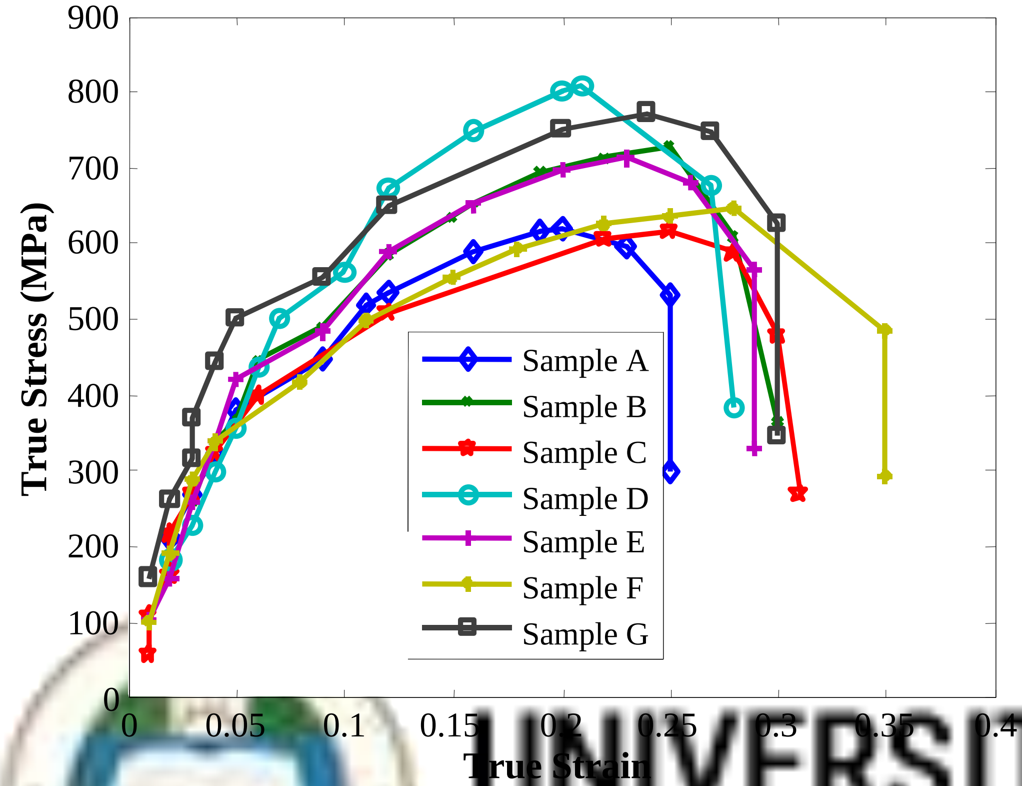

Figure 4.2 True Stress-Strain of Air-Cooled Rolled Bar

The non-metallic inclusions observed are a combination of tramp elements and slag that could not be removed at the refining stage of the steel making process. Melting of most inclusions is not feasible during the reheating of rolling stocks in the furnace, which operates around 1200^0 C. This is because basic slags that are mainly compounds of silica and magnesia are highly refractory being able to withstand above 1700 ^{0}C (Pickering, 1958). Such inclusions merely deform along the direction of rolling thus conferring directional properties on the rolled bars. Deformability of inclusions during hot working of steel influences the final properties of the product (Chunhui and Stahlberg, 2001). Deformed inclusions also distort normal grain boundary arrangements that are potential barriers to dislocation motion.

Specimen G exhibited a good combination of ultimate tensile strength, 773.2 MPa and elastic modulus, 19157.9 MPa being the highest amongst all specimens tested.

This may be attributed to two factors namely fairly low finishing temperature 855^{0}C, which gave rise to fine grained pearlite during air-cooling and low concentrations of inclusions, Ceq 0.38. Similar satisfactory performances were observed in specimens B and E having 728 and 711 MPa ultimate tensile strengths due to low finishing temperatures and low Ceq. The combination of these factors favours modest strain hardening during both elastic and plastic deformations.

4.1.3 Yield strength of air-cooled bar

The results of variation of yield property behaviour with finishing temperatures and carbon content are shown in Figures 4.3 and 4.4 respectively.

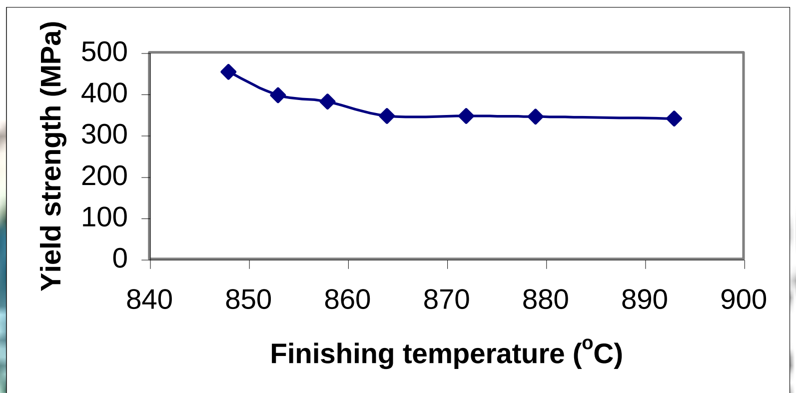

Figure 4.3 Yield strength against finishing temperature

Specimens A-F exhibited low yield strengths in the range 380.8-396 MPa. The yield strength of sample G, 452.8 MPa is comparable to local and international specifications, which are 420 MPa (NIS), 460 MPa (BS) and 500 MPa (ASTM). The yield point phenomenon common in steel, aluminium and copper, is associated with small amounts of interstitial or substitutional impurities (Smallman and Bishop, 1999). This partly accounts for the observed substantial ductility in low carbon steels having interstitial carbon concentrations between 0.1 and 0.25 per cent maximum. It has been shown (Hall, 1970) that almost complete removal of carbon and nitrogen from low carbon steel by wet-hydrogen treatment will remove the yield point phenomenon. However, only about 0.001 per cent of either of these elements is required for a reappearance of the yield point.

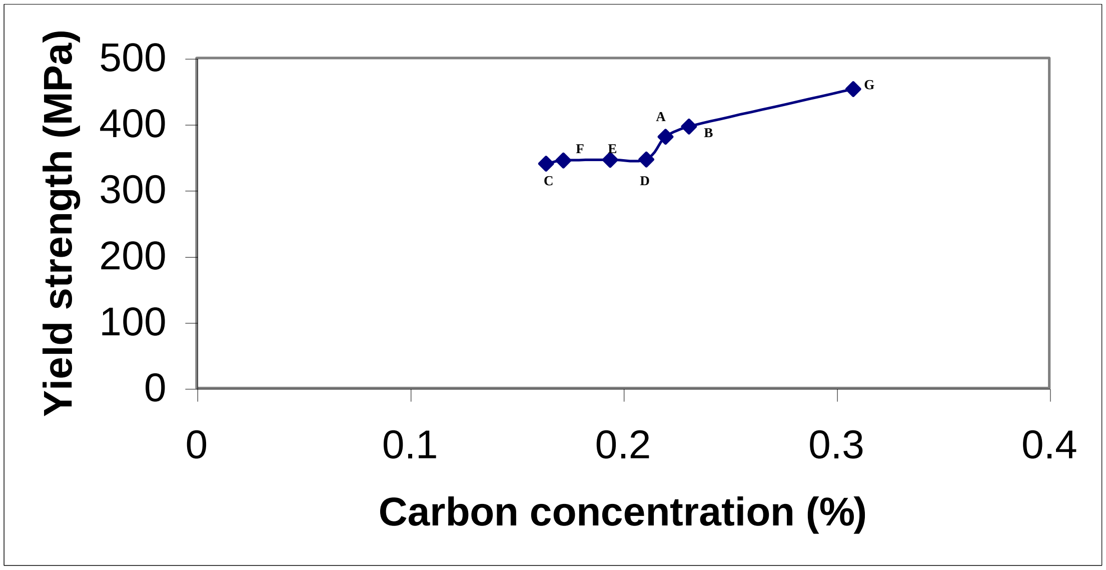

Figure 4.4 Variations of yield strength with carbon concentration.

Gradual increase in yield strength of test specimens occurred from 0.15 – 0.19 % carbon (see Figure 4.4). Sharp increase in yield strength was observed between 0.19 and 0.23% carbon with corresponding finishing temperature in the range 848^{o} – 858^{o}C. Above this temperature range (see Figure 4.3) and irrespective of the carbon composition, the yield strength dropped substantially. From this observation, it can be inferred that the type of microstructure developed at finishing temperatures greatly influenced the yield values obtained. Though specimen D has 0.30 % carbon, yet it exhibited merely yield strength of 344.8 MPa. Yielding phenomenon in low carbon steel peaked between 0.20 and 0.30 %C. Beyond this range; the ductility of carbon steel is impaired. Apart from weldability criterion, this may be another basis for the BS 4449 specification of 0.25% carbon maximum in billets/ingots employed in hot rolling of construction steel bars.

4.1.4 Hardness of air-cooled bars

Table 4.4 shows values of hardness induced in the steel bars after air-cooling. Hardness exhibited by the specimens varies with the carbon concentrations of rolling stock.

Table 4.4 Hardness of air-cooled steel bar

Specimen ID	Hardness measurements (HRB)*					Hardness Value (Ave)
	1	2	3	4	5	
A	73.1	71.8	72.4	73.9	72.3	72.7
B	84.6	85.2	84.1	82.8	84.8	84.3
C	61.8	61.4	61.7	63.1	62.5	62.1
D	91.6	93.3	94.6	93.8	92.7	93.2
E	86.9	88.1	87.2	85.9	87.4	87.1
F	67.3	68.5	68.9	67.7	67.6	67.8
G	87.2	86.1	85.8	86.7	86.2	86.4

***** Ball diameter: D 0.002mm, Specimen surface: Flat, Condition: Ambient temperature

Under natural air-cooling as is the case in this study and at such finishing temperature range 848^o – 893^{o}C, hardness developed on the bar's surface is in the range of 62.1-93.2 HRB (Figure 4.5). The hardness measured must have been induced entirely by cementite rather than martensite. This is because, martensite could not have formed given the prevailing processing conditions. Relevance of adequate surface hardness required in reinforcing bars concerns the ribs, which are meant to offer resistance to slip of the bar member within the structure. Free slip of bars should not be greater than 0.2mm in a pullout test (Rao, 1961). The ribs must therefore exhibit sufficient bond strength in order to function effectively.

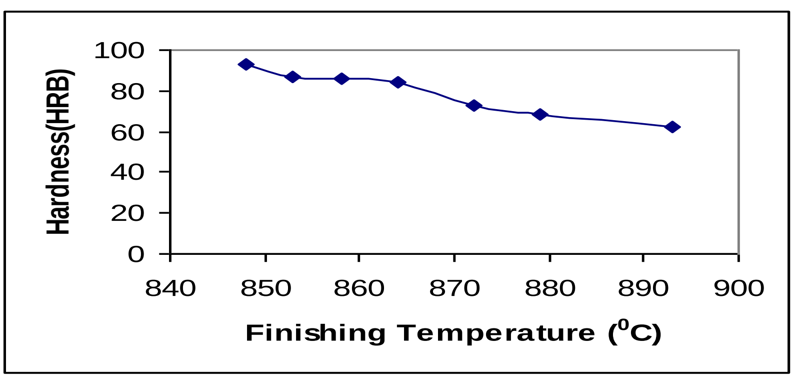

Figure 4.5 Variations of hardness with finishing temperature

4.2 Spray-quenched specimens' temperature profile

The variations of measured temperatures of the spray-quenched specimens are presented in Table 4.5. The data are plotted in Figure 4.6 which indicates the specimens' degree of under cooling within the period stipulated in the experiment.

Table 4.5 Temperature profile of spray-quenched specimens

Spray-Quench duration (SQ_d) s	Spray-Quench rate (SQ_r) ml/s	Cooling rate (T_r) $^0C/s$	Specimen temperature profile, SS_T (^0C) 0.2%$\pm$ 1°C						
			800	820	840	860	880	900	1000
5	40.0	118	212	233	251	269	288	311	410
10	20.0	65	165	172	201	209	234	255	352
15	13.3	47	113	121	135	168	182	204	301
20	10.0	36	98	102	128	143	168	189	282
25	8.0	28	91	113	124	137	155	176	272
30	6.0	24	73	92	112	126	141	168	267
40	5.0	18	71	87	104	121	136	152	253

Notations: SQ_d – Spray-quench duration(s): The **SQ_d** was preset for the experiment by synchronizing the theoretical and industrial time for obtaining desirable austenite decomposition products. **SS_T** – Specimens' temperature after quenching (^0C).
Tr – Cooling rate ($^0C/s$): Cooling rates were calculated using the **SS_T** data at the end of each spray quench cycle. **SQ_r** – Spray-quench rate (ml/s): Varied volume of water flow was obtained by varying the piping dimensions in and out of the water pump during each quenching cycle.

Mathematically, cooling rate, **Tr** is given as;

$$Tr = \frac{A_T - SS_T}{SQ_d} \quad (^oC/s) \qquad 4.1$$

Where A_T is the specimen autenitising temperature (°C), SS_T is specimen temperature after quenching and SQ_d is spray quenching duration (seconds).

Figure 4.6 shows the variations in the test specimens' temperatures profile at the end of each spray-quenching cycle. Specimens' temperatures profile decreased down each of the austenitising temperatures. This is due to time variations, which increases with successive cooling rates giving rise to additional cooling by natural effect. Given the observed temperature range of 71^0-410 ^{0}C, the efficiency of the cooling method adopted can be adjudged fairly adequate. This temperature range would have resulted in the formation of a mixture of lower bainite and martensite on the surface and pearlite in the core of test specimens. However, this was not the case with specimens austenitised between 880 ^{0} and 1000 ^{0}C and cooled in the range 24-18 ^{o}C/s. This is due to the rather long cooling duration (25-40 seconds).

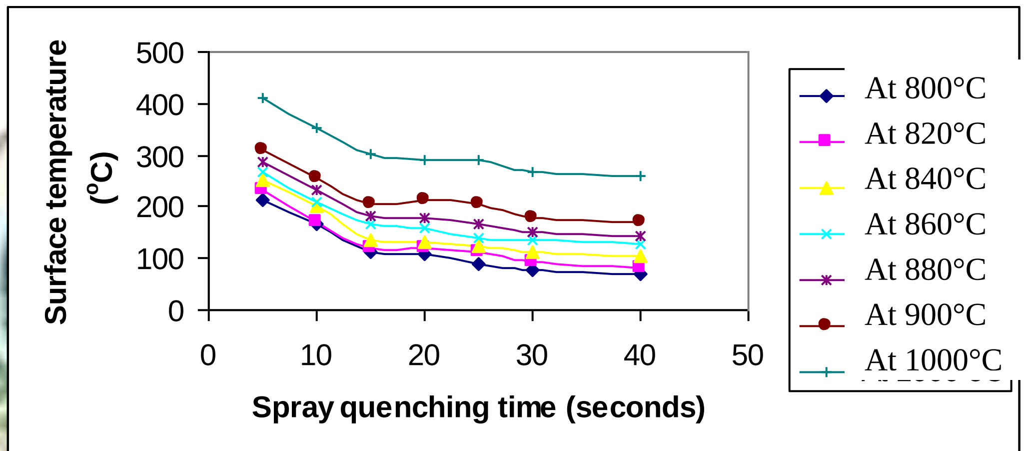

Figure 4.6 Variation of specimens temperature with spray quenching time

Within 800^{o}C-900^{0}C austenitisation range and quenching duration of 5 to 15 seconds, the specimens' temperatures, 113^{0}C-311 ^{0}C are sufficiently low for austenite transformation into a mixture of lower bainite and martensite to occur. Consequently, specimens treated under these conditions exhibited yield and ultimate strength values in the range of 633-842.8 MPa and 704.0 - 1173.6 MPa respectively. The hardness and impact toughness of the bars also improved considerably. This is expected (Vijendra, 2004) because, the greater the degree of under cooling of austenite the greater the propensity to transform.

4.2.1 Microstructural observation on spray quenched specimens

The microstructures developed in specimens after spray quenching at varying water flow rates are shown in Plates 4.2-4.4. The change in grain size, shape and distribution are seen to depend on the specimens' temperature profiles after spray quenching. Grain sizes (apparent) increased with decreasing cooling rates at each austenitising temperature. Lower bainite structure evolved in specimens spray quenched within 10 seconds as their temperatures were lowered to between 165^{0}Cand 261^{0}C. Similar low temperatures attained by other specimens could not induce lower bainitic phase due to a much longer cooling duration of 15-40 seconds.

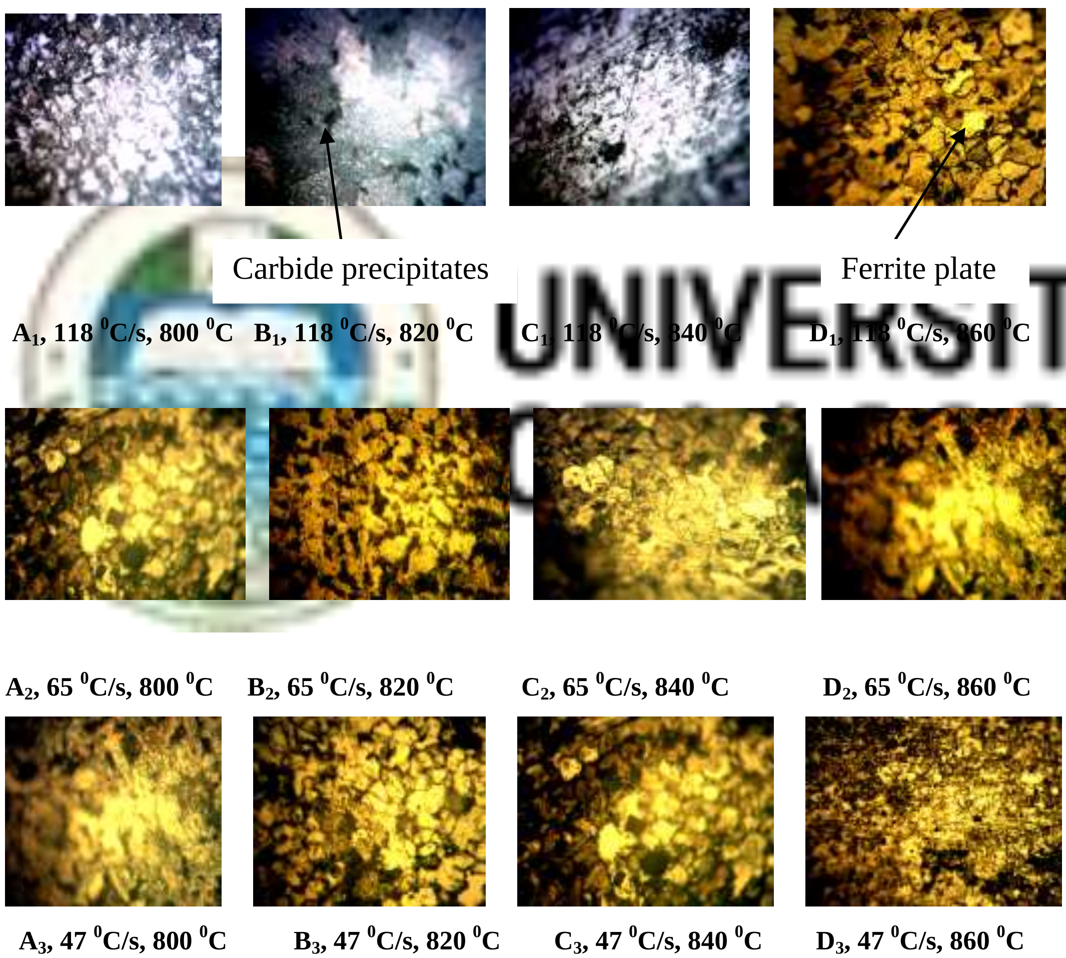

Plate 4.2 Micrographs of test specimens showing Lower Bainitic structure (x800)

Micrographs on **Plate 4.2 (A_1-A_3, B_1-B_3, C_1-C_3** and **D_1-D_3**) show lower bainitic microstructure formed in 12 of the specimens at the cooling rates of 118, 65 and 47 ^{0}C/s within 800^0-860^{0}C austenitising temperatures. The structure consists of carbide precipitates dispersed in a matrix of ferrite plates. Lower bainite microstructure is similar to tempered martensite and is capable of exhibiting comparable mechanical properties (Ohtani, et al, 2007). Fast under cooling of carbon steels from the austenitising temperature usually gives rise to decrease in the amount of proeutectoid phases present (Hong, et al, 2009). This is because more carbon tends to precipitate out of solution thereby enriching the transformed portion in carbon. This phenomenon occurs in a relatively short time for which such transformation is kinetically favourable.

Mixture of fine pearlite was observed in 23 specimens as shown in **Plate 4.3 (A_4-A_5, B_4-B_5, C_4-C_5, D_4-D_5, E_1-E_5, F_1-F_5** and **G_1-G_5**). This transformation occurred within two different cooling regimes; that of 118, 65 and 47^{0}C/s at 880^0-1000^{0}C and 36, 28 ^{0}C/s between 800^0 and 1000^{0}C austenitising temperatures respectively. The combination of delayed transformation (25 seconds) and a relatively low cooling rate are responsible for this transformation product.




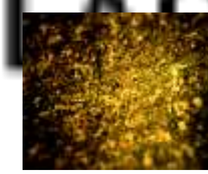
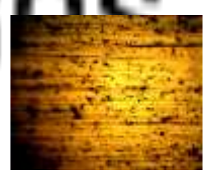

Fine cementite   Fine ferrite

E_1, 118 ^{0}C/s, 880 ^{0}C F_1, 118 ^{0}C/s, 900 G_1, 118 ^{0}C/s, 1000 ^{0}C E_2, 65 ^{0}C/s, 880 ^{0}C F_2, 65 ^{0}C/s, 900^{0}C



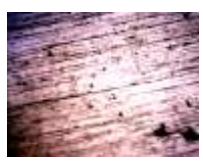

G_2, 65 ^{0}C/s, 1000^{0}C E_3, 47 ^{0}C/s, 880^{0}C F_3, 47 ^{0}C/s, 900^{0}C G_3, 47 ^{0}C/s, 1000^{0}C A_4, 35 ^{0}C/s, 800 ^{0}C





B_4, 35 ^{0}C/s, 820 ^{0}C C_4, 35 ^{0}C/s, 840 ^{0}C D_4, 35 ^{0}C/s, 860 ^{0}C E_4, 35 ^{0}C/s, 880 ^{0}C F_4, 35 ^{0}C/s, 900^{0}C





G_4, 35 ^{0}C/s, 1000^{0}C A_5, 28 ^{0}C/s, 800 ^{0}C B_5, 28 ^{0}C/s, 820 ^{0}C C_5, 28 ^{0}C/s, 840 ^{0}C D_5, 28 ^{0}C/s, 860 ^{0}C.



E_5, 28 ^{0}C/s, 880 ^{0}C F_5, 28 ^{0}C/s, 900^{0}C G_5, 28 ^{0}C/s, 1000^{0}C

Plate 4.3 Micrographs of test specimens showing fine Pearlitic structure (x800).

Further decrease in cooling rate, 24 and 18 ^{0}C/s and longer duration of spray quenching gave rise to coarse pearlite at all austenitising temperatures. This is evident in the 14 micrographs on **Plate 4.4** (**A_6-A_7, B_6-B_7, C_6-C_7, D_6-D_7, E_6-E_7, F_6-F_7** and **G_6-G_7**). Coarse pearlite degrades the specimens' hardness, yield strength, ductility and impact toughness. The foregoing microstructural observations are indicative of time and temperature dependence of austenite transformation in plain carbon steel.

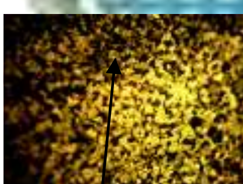


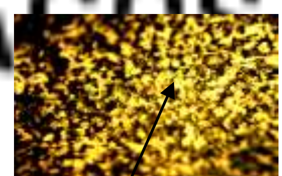

Coarse ferrite

Coarse cementite

A_6, 19 ^{0}C/s, 800 ^{0}C B_6, 19 ^{0}C/s, 820 ^{0}C C_6, 19 ^{0}C/s, 840 ^{0}C D_6, 19 ^{0}C/s, 860 ^{0}C



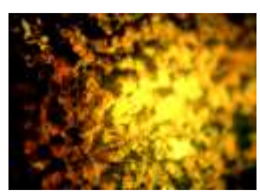
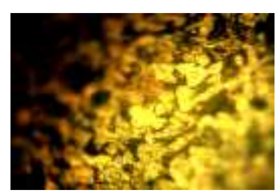

E_6, 19 ^{0}C/s, 880 ^{0}C F_6, 19 ^{0}C/s, 900^{0}C G_6, 19 ^{0}C/s, 1000^{0}C A_7, 13 ^{0}C/s, 800 ^{0}C



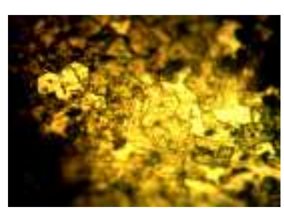


B_7, 13 ^{0}C/s, 820 ^{0}C C_7, 13 ^{0}C/s, 840 ^{0}C D_7, 13 ^{0}C/s, 860 ^{0}C E_7, 13 ^{0}C/s, 880 ^{0}C

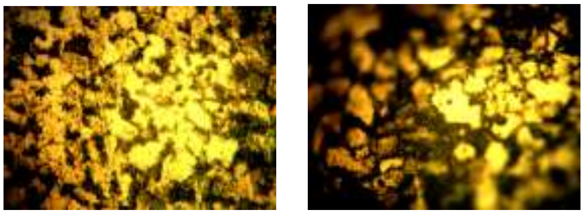

F_7, 13 ^{0}C/s, 900^{0}C **G_7, 13 ^{0}C/s, 1000^{0}C**

Plate 4.4 Micrographs of test specimens showing coarse Pearlitic structure (x 800).

4.2.2 Ultimate tensile strength of spray-quenched specimens

Figures 4.7-4.13 show the true stress-strain curves of air-cooled and spray-quenched test specimens. The curves indicate that the effect of increased cooling rates by spray quenching is quite significant. Details of the tensile test and impact energy results of the spray-quenched specimens are presented in Appendix C (C1-C8).

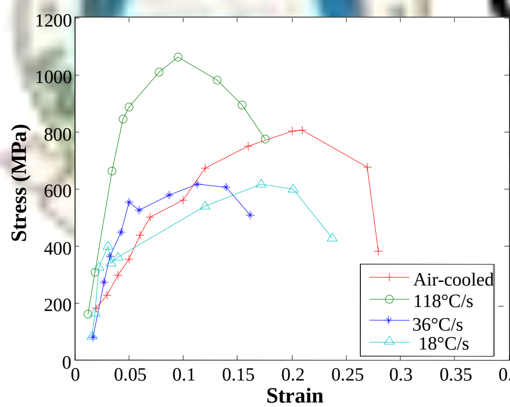

Figure 4.7 True stress-strain flow curves of air-cooled and spray-quenched specimen austenitised at 800^{0}C

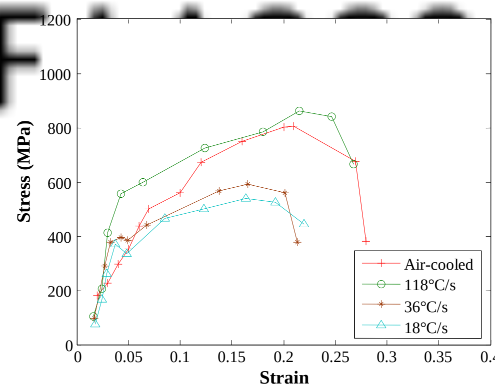

Figure 4.8 True stress-strain flow curves of air-cooled and spray-quenched specimen austenitised at 820^{0}C

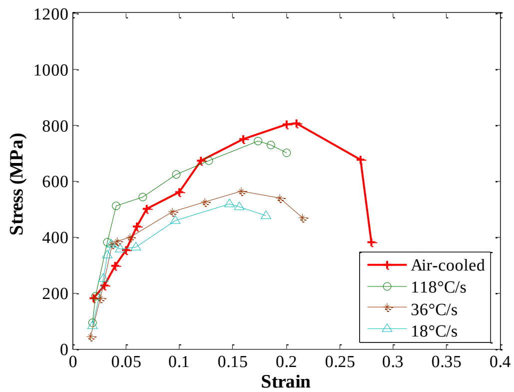

Figure 4.9 True stress-strain flow curves of air-cooled and spray-quenched specimen austenitised at 840^{o}C

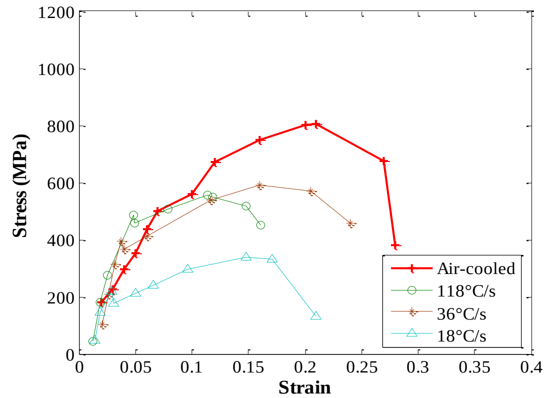

Figure 4.10 True stress-strain flow curves of air-cooled and spray-quenched specimen austenitised at 860^{o}C

Spray-quenched specimens exhibited ultimate tensile strength in the range, 704-1173 MPa compared with 616.7-806.9 MPa of conventional steel bar (Figure 4.7–4.10). This represents a mark-up of 31.9% in strength. This occurred between 47 and 118^{0}C/s cooling rates and corresponding austenitising temperatures are in the range 800^{0}-860^{0}C within 15 seconds maximum spraying duration. Substantial increase in ultimate tensile strength can be explained in terms of the differing morphologies and textures of pearlite and lower bainite. Pearlite is composed of alternate plates of ferrite and cementite with the thickness of the plate determining the grain size. In contrast, lower bainite comprises precipitates of carbide in ferrite plate matrix. The carbide precipitates act as barrier to dislocation motion hence, increase in ultimate tensile strength.

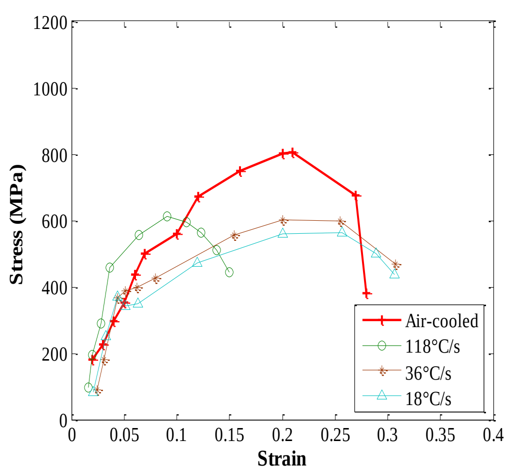

Figure 4.11 True stress-strain flow curves of air-cooled and spray-quenched specimen austenitised at 880^{o}C

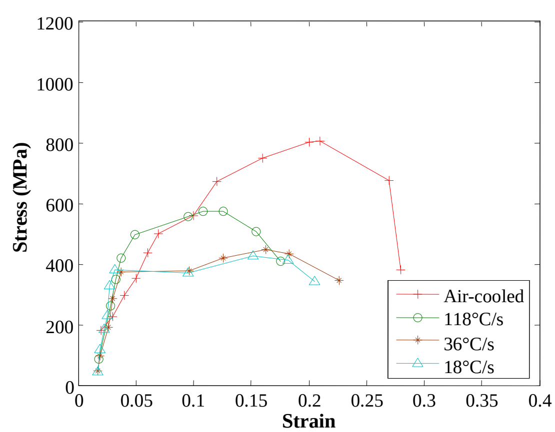

Figure 4.12 True stress-strain flow curves of air-cooled and spray-quenched specimen austenitised at 900^{o}C

However, sharp departure from the above was observed at higher heat treatment temperatures (880^0-1000^{0}C) and longer time, 20-40 seconds of spray quenching. The resulting ultimate tensile strength values dropped to the range 340.0-625.7MPa (Figure 4.11 – 4.13). This is indicative of the negative effect of delayed transformation of austenite whereby high volume fraction of coarse pearlite is formed (Bontcheva and Petzov, 2005). Worth noting however, is the exceptionally high strength induced in the specimen at 800 ^{0}C within the cooling rates of 47, 65 and 118 ^{0}C/s. This can be attributed to the high volume fraction of carbide precipitates formed under this condition.

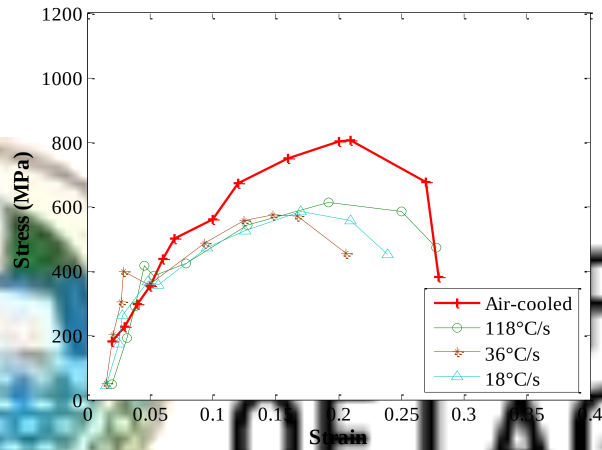

Figure 4.13 True stress-strain flow curves of air-cooled and spray-quenched specimen austenitised at 1000^{o}C

4.2.3 Modulus (Stiffness) of spray quenched specimens

The Young’s modulus of elasticity value (**€**) expresses the amount of stress necessary to produce unit elastic strain (Higgins, 1985). This value is directly related to the materials stiffness, which is a primary design consideration in structural calculations (Tietz, 1984). One of the quality requirements of a good reinforcing steel bar is the possession of adequate level of stiffness to guard against excessive deflection of structures. Superfluous deflection often renders reinforcing steels defective especially in such applications as in high-rise buildings and bridges.

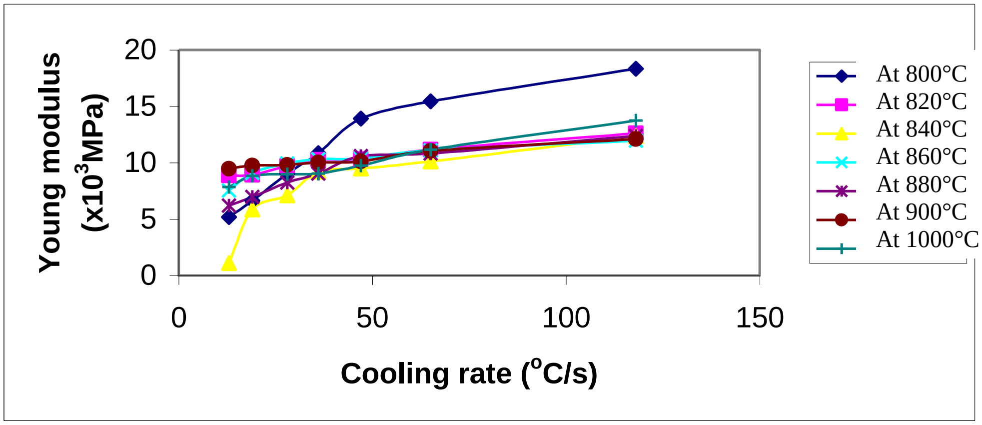

Figure 4.14 Variation of stiffness induced in specimen at varying cooling rates

Figure 4.14 drawn from the data in Table D2 (Appendix D) shows that test specimens' elastic strain variations follow similar trend observed with the yield strength. This is expected because stiffness is induced in a material to the extent of bond cohesion within the crystals, which is a function of microstructural texture. Stiffness property is often affected by the presence of impurities, inclusions and defects in the materials microstructure.

4.2.4 Ductility of spray quenched specimens

The amount of plastic strain suffered by the material before fracture corresponds to its ductility measured in percent elongation (%) at fracture. Good quality construction steel must possess appropriate level of ductility for an enhanced formability. Table D4 (Appendix D) contains data on ductility variations of spray-quenched specimens. All the test specimens exhibited adequate ductility having manifested this property in the range 15.0 -32.9% (Figure 4.15) compared with 28.2-41.9% in conventional bar. Again, the preponderance of carbide precipitates in the microstructure is responsible for the marginal reduction in ductility.

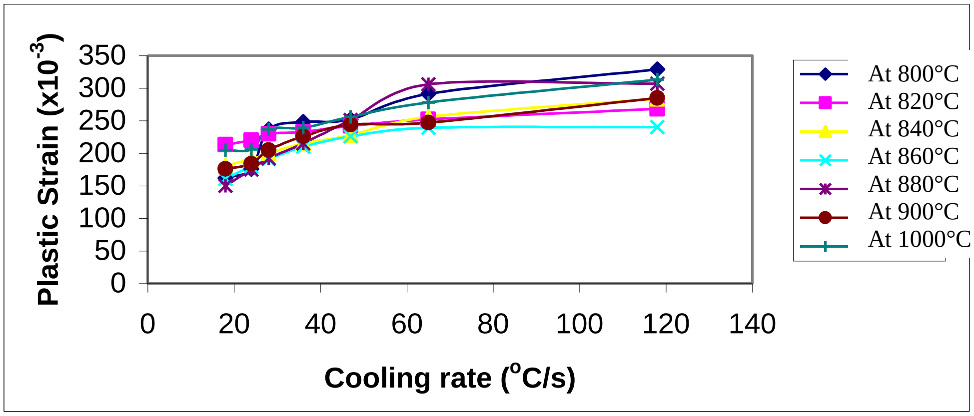

Figure 4.15 Plasticity property of spray-quenched specimens at varying cooling rates

The minimum standard elongation for the steel bar under investigation is 10% of test specimen gauge length. It must be noted however, that beyond 35% elongation, the ductility becomes superfluous and the material is too soft to be used for reinforcement purposes.

4.2.5 Impact toughness of spray quenched specimens

Sudden forces such as thunderstorms, seismic waves and irregular loading in the case of bridges, impact most structures. Reinforcing steel bars are therefore required to possess adequate toughness under such conditions to prevent brittle failure. Figure 4.16 shows the impact toughness behaviours of test specimens according to the data in Table D3 (Appendix D).

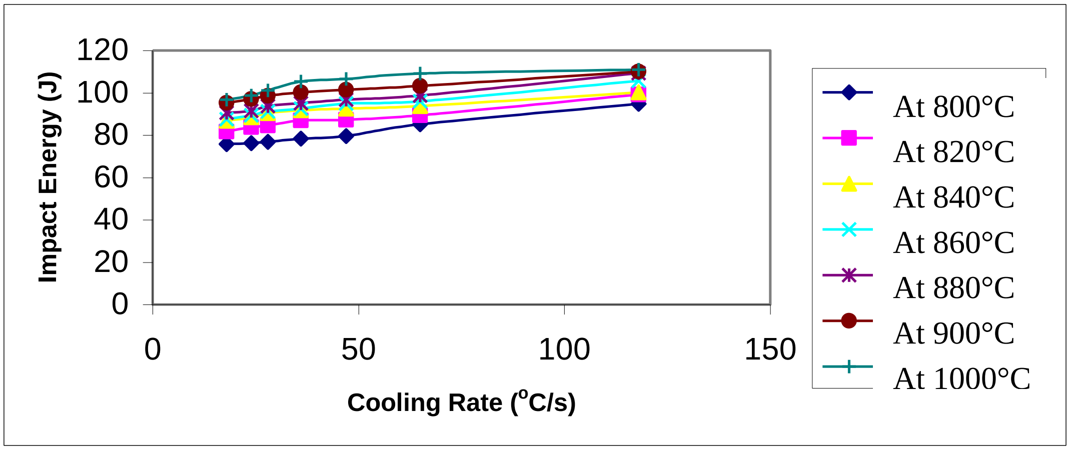

Figure 4.16 Impact energy of spray-quenched specimens at varying cooling rates

The obvious similarity in the pattern of toughness property of spray-quenched specimens and the plastic strain curves (Figure 4.15) shows that toughness encompasses strength and ductility. This is expected because the amount of energy absorbed to break inter-atomic bonds between grains corresponds to the extent of plastic deformation suffered by test specimens (Tan, et al, 2008). In the final analysis, spray quenched specimens exhibited higher impact energy; 85.2-111.0 **J** compared with the as-rolled 78.4-82.0 **J** thereby enhancing the material toughness.

4.2.6 Hardness of spray quenched specimens

Reasonable surface hardness is required in reinforcing bars in order to achieve adequate bond strength at the bar and concrete interface for prevention of slip. Bond strength is considered to have failed when the relative slip is 0.127-0.254mm (Rao, 1961). Occurrence of slip usually gives rise to the failure in the adhesion between the reinforcement and the concrete interface. The bar ribs must therefore exhibit sufficient wear resistance in order to function effectively.

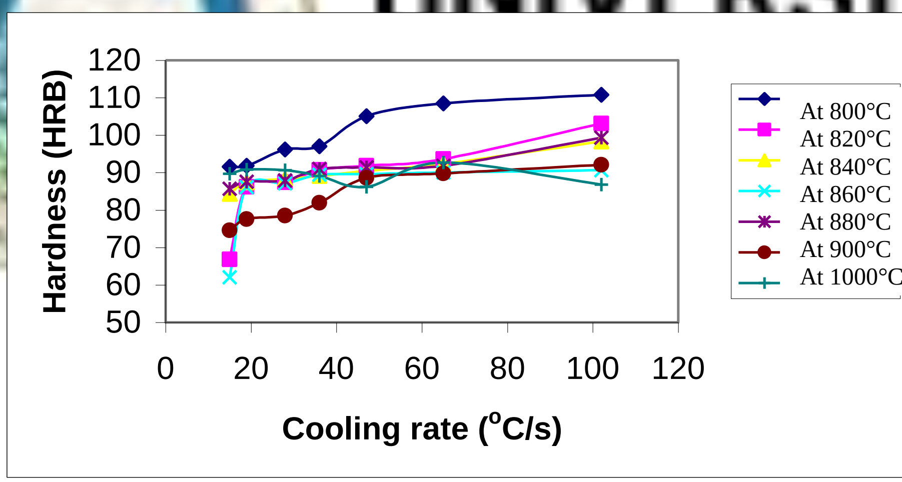

Figure 4.17 Hardness of spray-quenched specimens at varying cooling rates

Table D5 (Appendix D) contains the data on micro-hardness induced in the spray-quenched specimens. Specimens at all austenitisation temperatures but within 47 to 118 ^{0}C/s cooling rates show increased hardness (Figure 4.17) in the range of 84.3-110.8 HRB compared with that obtained in conventional bar, 62.1-93.7 HRB. The hardness level exhibited by the spray-quenched specimens further confirms that lower bainite share some microstructural similarities with tempered martensite.

4.2.7 Yield strength of spray quenched specimens

Yielding of ductile material such as steel produces permanent deformation (Kempter, 1979) hence, the importance of yield stress as a critical design parameter in engineering.

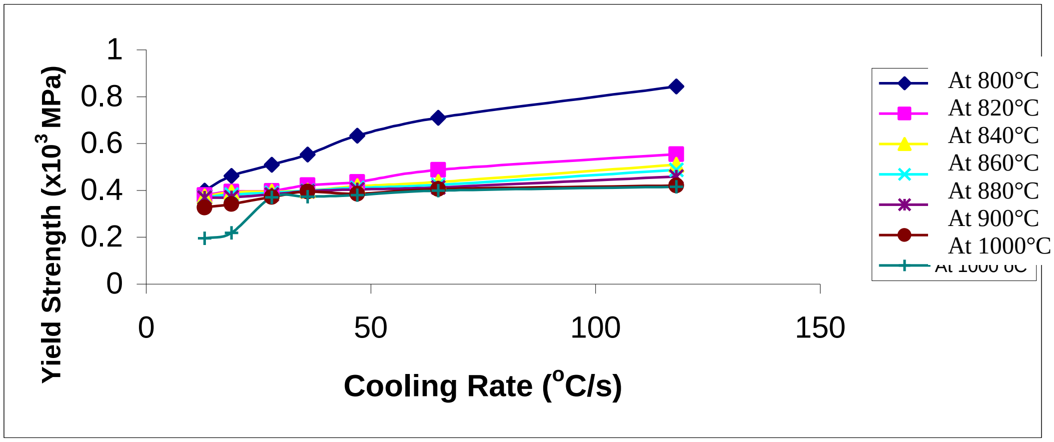

Figure 4.18 Yield strength property at varying cooling rate

The data in Table D (Appendix D) were used to draw the curves in Figure 4.18. It is observed (Figure 4.18) that specimens subjected to cooling rates 47, 65 and 118 ^{0}C/s of 800^0-880^{0}C treatment temperatures exhibited yield strength in the range 421.9-842.8MPa compared with 340.1-452.8MPa obtained in conventional bars. This development represents an increase of 59.5% in yield strength. This range of yield strength conforms to local and international standard specifications, which are 420MPa (**NIS**), 460MPa (**BS**) and 500MPa (**ASTM**).

The concept of yield in low carbon steels depends heavily on the presence of small interstitial atoms such as carbon, boron, and nitrogen. The amount and distribution of any of these interstitial atoms govern the yield behaviour of the material (Hall, 1970). Increase in yield property of test specimens can therefore be explained in terms of the texture of lower bainite. Carbide precipitates act as interstitial elements in addition to the carbon in solution and these enhance the yield strength of test specimens. Generally, the yield strength of steels increases with decreasing bainite carbide grain size as established by the Hall-Petch relationship. The carbide precipitates are orientated as low angle sub-grain boundaries, which act as barriers to dislocation motion contributing significantly to the strength of lower bainite.

4.3 BAINITIC YIELD STRENGTH-BAND FOR SPRAY-QUENCHED STEEL

The development of a property band generally facilitates the selection of process variable range within which desirable mechanical properties can be achieved. The information obtained from such a chart are useful in taking critical technological decision. Property band also enhances in-process quality control. Figure 4.19 shows the Bainitic yield strength band developed from the results of yield strength values obtained in this study.

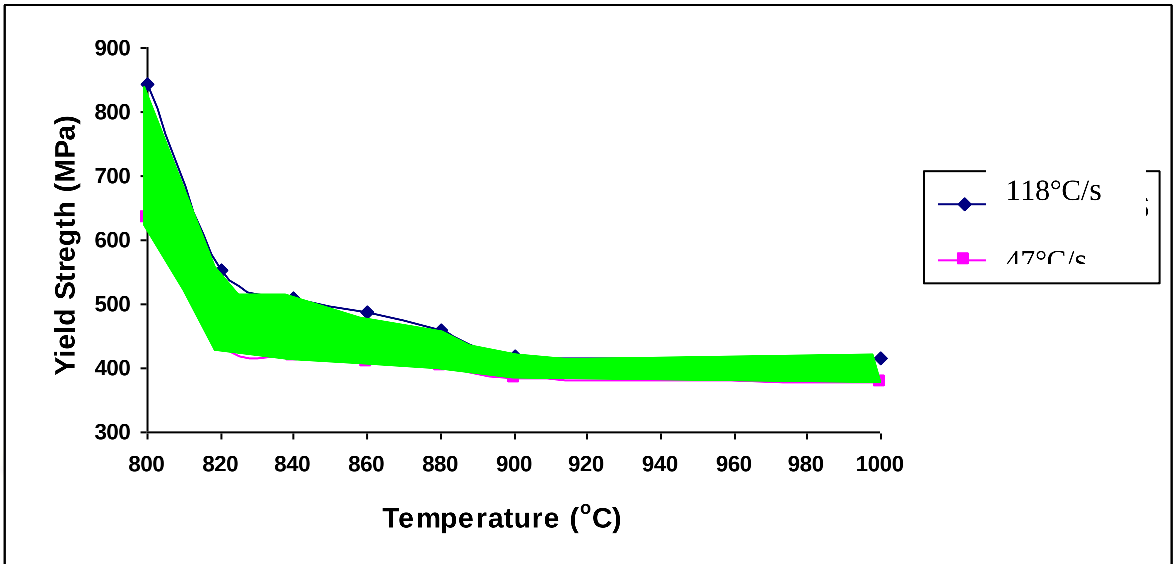

Figure 4.19 Bainitic yield strength band for spray-quenched hot rolled steel

The processing variables employed are temperature and cooling rate. The chart illustrates the variations of temperature and cooling rates and the yield strength developed within the lower and the upper limits of both variables. Between 800° and 880°C and cooling rates of 47, 65 and 118°C/s, yield strength values are within standard specifications (**NIS**, **BS** and **ASTM**). In the temperature range of 900°-1000°C however, the cooling rate must be close to 118 °C/s for steel of desirable yield strength to be produced.

4.4 PREDICTING YIELD STRENGTH AT VARYING COOLING RATES

The decisive importance of yield strength property, σ, that a construction steel bar is expected to exhibit necessitates a prior production prediction of its attainment at given processing conditions. Using the yield strength property test result data obtained in this study (Appendix D, Table D1), an empirical model was developed through Newton-divided difference method to predict yield strength at any cooling rate in the range of 18-118^{0}C/s prior production. The generalised empirical model is given as:

$$\sigma = \alpha T_R^{\ 6} + \beta T_R^{\ 5} + \delta T_R^{\ 4} + \theta T_R^{\ 3} + \gamma T_R^{\ 2} + \lambda T_R + \eta$$

Where T_R is the cooling rate (ºC/s), **α, β, δ, θ, γ, λ** and **η** are constants and their values (Table 4.6) at varying austenitising temperatures were obtained using Mathcad software.

Table 4.6: Empirical model constants values

Temp. ºC / Constant	800	820	840	860	880	900	1000
α (MPa.s^6/^{o}C^6)	7.157×10^{-7}	2.244×10^{-7}	1.401×10^{-8}	4.765×10^{-8}	1.731×10^{-7}	4.597×10^{-7}	4.7507×10^{-6}
β (MPa.s^5/^{o}C^5)	-2.186×10^{-4}	-6465×10^{-5}	-2.561×10^{-6}	-1.431×10^{-5}	5.444×10^{-5}	-1.468×10^{-4}	-1.4751×10^{-3}
δ (MPa.s^4/^{o}C^4)	2.539×10^{-2}	6.884×10^{-3}	2.041×10^{-5}	1.621×10^{-3}	6.585×10^{-3}	1.802×10^{-2}	1.5055×10^{-1}
θ (MPa.s^3/^{o}C^3)	-1.449	-3.507×10^{-1}	1.933×10^{-2}	-8.945×10^{-2}	-3.966	-1.098	-10.269
γ (MPa.s^2/^{o}C^2)	43.123	9.339	-1.333	2.526	12.551	34.982	315.592
λ (MPa.s/^{o}C)	-626.839	-137.940	34.309	-32.861	-197.656	-549.662	-4821.864
η (MPa)	3887.349	1503.972	78.913	519.665	1603.958	3657.184	28877.121

Based on the array of data in Table 4.6, the yield strength of rolled bar in-process can be predicted under any set of finishing temperature and cooling rate conditions. The model can also be employed in writing of a set of computer algorithms for the end-operation activities of the rolling process. This is capable of facilitating automation of the conventional rolling and cooling requirement for efficient attainment of desirable yield strength property of the steel bar. However, the empirical model is applicable to only the category and size range, 12-32mm of steel bars covered by this study in the as-rolled condition.

CHAPTER FIVE

5.0 CONCLUSION

The complex interactions between thermal, mechanical and metallurgical phenomena in conventional hot rolled high yield steel bars have been investigated. In-depth review of the impact of these parameters on the strength characteristics of the rolled steel was also carried out. Significant improvement was achieved both in processing method and in the basic functional properties of the rolled bars.

5.1 Summary of Findings

On the basis of results obtained and their analyses, the following conclusions can be drawn:

5.1.1 Finishing Temperature

In hot rolling, temperature at the last pass greatly influences microstructure and mechanical properties of the final product. The level of inter-stand temperatures also affect metallurgical phenomena such as strain, strain rate and recrystallisation (static and dynamic) to the extent that in-process austenite grain size is altered. Direct correlation exists between roll stock austenite grain size and that of the rolled product. This must be controlled to prevent impairment of rolled product mechanical properties. In this work, finishing temperature varied widely in the range 848–893^{o}C. This is high enough to induce grain coarsening in conventional rolling where the products are air-cooled on the Run out Table (ROT). Hence, finishing temperature must be kept low, around 140^{o}C above A_1 (723^{o}C). Avoidance of excessive grain growth phenomenon during thermomechanical processing is ensured by strict adherence to heat treatment rules governing ideal soaking time for roll stocks and control of cooling regime of the final product.

5.1.2 Cooling Regime and Microstructure

Obvious differences between the microstructures of specimens air-cooled (see Plate 4.1) and those spray-quenched (see Plates 4.2-4.4) have shown that cooling rate has great influence on the microstructures developed in rolled products. The most significant aspect of the influence has been observed in the morphologies of the transformed phases.

While the air-cooled specimens developed pearlite consisting of alternate plates of ferrite and cementite (α, Fe_3C) mainly, spray-quenched specimens exhibited a mixture of lower bainite and pearlite. Lower bainite morphology being a dispersion of carbide precipitates in ferrite plates presents significant improvement on the pearlitic structure. Thus, spray quenching is an alternative method of fast undercooling, which induces microstructures that confer improved mechanical properties. The time taken at spray quenching of rolled product on the cooling bed must be controlled as it affects diffusion dependent austenite decomposition into lower bainite.

5.1.3 Yield Strength

Yield strength is the basic material performance parameter in engineering design. Specimens in which lower bainite was induced at cooling rates 47, 65 and 118 $^{o}C/s$ exhibited remarkable improvement in their yield strength, 422-843 MPa compared with 340-453 MPa in air-cooled specimens. The former values compared favourably with those obtained in dual-phase plain carbon steel, 450-550 MPa developed through solid solution hardening (Ray, et al 1997). This indicates that enhanced elastic property of rolled products is feasible in conventional rolling if the cooling rate is above that of air-cooling.

5.1.4 Ultimate Tensile Strength

Spray-quenched specimens exhibited improved tensile strength in the range of 704-1173 MPa in contrast to 616-807 MPa observed in air-cooled specimens. The relatively high degree of strengthening observed is attributable to the dispersion of carbide precipitates in the matrix of fine ferrite plates (Plate 4.2). This morphology is normally associated with high dislocation densities with the capacity to pin-down grain boundary motions giving rise to increased strength. This phenomenon occurred without impairment of ductility, which is in the range 15-33% in this work. Moderate ductility will stem the incident of undesirable deflection in structures such as beams, columns and scaffolds.

5.1.5 Impact Toughness

The ability to withstand brittle failure under dynamic loading of structures is one of the most important performance criteria of reinforcing steel. Spray-quenched specimens exhibited improved impact toughness because of the peculiar morphology of lower bainite in which ferrite plates act in a manner that inhibits crack propagation across any appreciable inter atomic distance within the matrix. This property is indicated by the amount of energy absolved prior to failure during test. The value obtained in this work is in the range of 85-111J compared with 78-82J of air-cooled samples, 80-120J being the standard specified.

5.1.6 Effect of Rolled Stock Composition

Appropriate elemental composition of roll stocks has complimentary influence on the strength characteristics of reinforcing steel. The results of this study have shown that mild steel stock composition in the range of 0.20-0.25%C, 0.18-0.20%Si, 0.05%S; 0.05%P, 0.45-0.80% Mn and 0.25%Cu max is preferable. This compared well with both the NIS 117: 2004 and BS 4449:1988 roll stock elemental specifications. The level of internal cleanness of roll stock should also be controlled by appropriate dilution of charges in terms of mixing heterogeneous scraps with directly reduced iron (DRI), briquettes and sinters. Incidence of heavily textured rolled products with its attendant anisotropy is greatly reduced through this practice.

5.2 Contribution to Knowledge

Inspite of enormous progress made in respect of strength characteristics enhancement in rolled products through thermomechanical processes, there still exists a neglect of establishment of appropriate process variables for the conventional hot rolling. This has made the problem of abysmally low strength characteristics of conventional hot rolled steel seem intractable. Relevant metallurgical and process parameters in terms of temperatures, strain, strain-rate recrystallization and cooling rate as they affect strength of hot rolled mild steel have been investigated. The results obtained compared very well with both results of previous works and the procedures developed produced steels which complied with all relevant standard specifications.

In summary, this study makes the following contributions to knowledge.

(i) The study establishes appropriate finishing temperature range, 800^o-860^oC, for conventional hot rolling.

(ii) Unique cooling rate range of 47-$118^oC/s$, capable of inducing the type of microstructure that gives rise to improved strength was established.

(iii) A new microstructure, lower bainite, instead of conventional pearlite was developed in hot rolled steel bar through spray quenching.

(iv) The study provides for yield band chart and empirical model, which are extremely useful for in-process quality control and prediction of yield strength of hot rolled steel bars.

5.3 RECOMMENDATION

The future of the steel industry is linked to its technological progress in terms of reducing cost and improving product mechanical properties. These are achievable through technical innovation which gives rise to new process technology. The inducement of bainitic structure in the steel bar constitutes a significant improvement in processing method in the steel industry, which has resulted in production of steel bars with strengths conforming to international standards. To facilitate adoption of the research findings in the steel industry, the following recommendations are made:

- Rolling stocks, billets/ingots should be cast from semi-killed molten steel in which the volume of oxygen and other dissolved gases are $\leq$ 30 ppm. Where the stocks are imported, they should be accompanied by quality certificate indicating clearly the internal cleanness status.
- Based on the heterogeneous nature of metal scraps used as major charges, thorough refining is required during melting; hence the Electric Arc Furnace (EAF) is most suitable. Induction furnaces used by some facilities in the industry will lead to the production of steels that are heavily impregnated with impurities such as slag, tramps and oxides.
- Clear distinction should be made between roll-stocks chemical composition meant for low and high-yield bars. Proper identification by batch numbering will enhance traceability of the stocks prior to charging into reheat furnace at rolling mill.

The current practice of using billets/ingots irrespective of the grade of rolled product intended should be discarded.

- Temperature monitoring devices namely pyrometers and thermocouples should be installed at intermediate and finishing stands. This will furnish prompt information on the extent of in-process cooling requirement. It will also ensure that rolled bars arrive cooling bed at temperatures a few degrees above A_1 point (723 ^{0}C) for efficient microstructural transformation through spray quenching.
- Relevant physical features such as ribs and flanges of appropriate width and height are almost non-existent on rolled steel bars produced in Nigeria. This is as a result of using worn-out roll grooves. These features are meant to compliment the strength of the bar and also enhance interfacial bond between the bar and concrete mixture. It is therefore recommended that tooling of roll grooves be carried out at predetermined tonnage of production. Three hundred (300) metric tones of rolled steel bars is recommended for reconditioning of roll grooves (Technical Bulletin, 1998).
- Steel rolling companies should be encouraged to procure relevant quality control/assurance equipment and also engage the services of qualified personnel to manage such facilities.
- Standards Organisation of Nigeria (SON) should intensify surveillance of operations in the steel industry and ensure compliance with above recommendations.

REFERENCES

Ahlborg, K. (1997): "Relationship between Ladle Furnace Slag-oxygen Potential and Contamination of Alumina Inclusions by MgO and CaO". Proceedings, 5th International Conference on clean steel, Hungary, pp.151-156.

Akiyama, M., Kuboki, T., Oikawa, K., Matsui, K. and Terada, K. (2002): "Influence of Carbon Content and Carbide Morphorlogy of Carbon Steels on Stress Strain Curve in Vicinity of Yield Point". Materials Science and Technology, vol.18, No.11, pp.1272-1278.

Alamu, D. J., Aiyedun, P. O., Kareem, A. and Waheed, M. A. (2007): "Effect of AISI 316 Stainless Steel Geometry on Temperature Distribution during Hot Rolling at High Reduction". Journal of Advanced Materials Research, vol. 18-19, pp. 195-200.

Alberto, A. (1995): "Direct Rolling of Slabs and Round Bars". Metallurgical and Plant Technology, vol.18, No.3, pp.60-64.

Appleton, E. and Summad, E. (2000): "2nd European Rolling Conference"; At AROS Congress Centre, Sweden, pp.24-26

Arvedi, G. and Guidani, A. (2004): "Metallurgical Based Development of Dual Phase Thin Hot Strip",;Acciaena Arvedi S. P. A., Ceremona, Italy, pp. 1-2.

ASTM (1973): Annual Book of ASTM Standards, Part 4 (Standards for Deformed Steel Bar)-A615- 72, A617-72, (1973, pp.684-699.

Augusti, A (1998): "Thermomechanical Rolling and Sizing in a Bar Mill". Steel Times International, vol.225, No.6, pp.44-59.

Bai, Y.G., Liu, C.M., Ren, H.P. and Zhang, X.G. (2003): "Microstructure and Mechanical Properties of High Strength Finishing Rolling Rebars". Journal of Northeastern University, Natural Science (China), vol.24, No.3, pp.268-271.

Balogun, S.A. (1974): "Determination of Deformation Forces in Cavity Press Forging". Journal of Metals Technology, MT/149, pp. 375-380.

Balogun, S.,Esezobor, D., Adeosun, S. and Sekunowo, O. (2009): "Challenges of Producing Quality Construction Steel Bars in West Africa: Case Study of the Nigeria Steel Industry". Journal of Mineral and Materials Characterisation and Engineering, vol.8, No. 4, pp. 283-292.

Barrett, C.S. and Massalaki, T.B. (1966): "Structure of Metals". 3rd Edition, McGraw Hill, New York, pp.82-96.

Bergstrom, Y. (1983): "The Plastic Deformation of Metals-A Dislocaton Model and its Applicability". Reviews on Powder Metallurgy and Ceramics, vol.2, pp.79-265.

Bontcheva, N. and Petzov, G. (2005): "Total Simulation Model of the Thermo-mechanical Process in Shape Rolling of Steel Rods". Computational Materials Science, vol.34, Issue4, pp.377-388.

Bowering, R. E. (1968): "The Microstructure and Mechanical Properties of Rolled Rods Controlled Cooled on a Moving Conveyor". p.65.

Bramfitt, B.L., and Speer, J.G. (1990): "Aperspective on the Morphology". Metallurgical and Materials Transactions A, vol.21, No.3, pp.817-829.

British Standards Specification (1988): "Carbon Steel Bars for the Reinforcement of Concrete". BS 4449, pp.4-8.

Charles, K. Kankam and Mark Adom-Asamoah (2002): "Strength and Ductility Characteristics of Reinforcing Steel Bars Milled from Scrap Metals". Materials and Design, vol.23, pp.537-545.

Choi, Y. and Kertesz, M. (2002): "Integrated Model for Thermo Mechanical Controlled Process in Bar Rolling". Materials Processing Technology, vol. 125-126, pp.678-688.

Chunhui, L. and Stahlberg, U. (2001): "Deformation of Inclusions During Hot Rolling of Steels": Journal of Materials Processing Technology, vol.114, pp.87-96.

Cuddy, L. J. (1984): "Grain Refinement by Control of Recrystallisation during Hot Rolling". Metallurgical and Materials Transactions A, vol.15, No.1, pp.87-98.

Curtin, W. A. and Dewald, M. (2005): "Multiscale Modelling of Dislocation/Grain Boundary Interactions". Session V34, Multiscale Phenomena for Fluid and Solids, pg. 520A.

De Hoff, R.T. (1968): "Quantitative Microstructural Analysis". American Society for Tests and Materials (ASTM) Specifications. Technical Publication 430, pp.63-95.

Dieter E. George (1976): "Mechanical Metallurgy". McGraw Hill Book Company, SI Metric Edition, pp. 145-240.

Dotreppe, J. C. (2006): "Mechanical Properties of Quenched and Self-Tempered Reinforcing Steel at Elevated Temperatures compared with Recommendations of Eurocode 2, Part 1-2". Journal of Materials and Structures, vol.30, No.7, pp.430-438.

Edmonds, D.V. and Cochrane, R.C. (1990): "Structur-Property Relationships in Bainitic Steels". Metallurgical and Materials Transactions A, vol.21, No.6, pp.1527-1540.

Elmer, J. W., Allen, S. M. and Eager, T. W. (1989): "Microstructural Development during Solidification of Stainless Steel Alloys". Metallurgical Transactions A, vol.20A, No.10, pp. 2117-2131.

Fapiano, D. Michael, S. and Smith, R. (2001): "Temperature Control in Hot Strip Mill". General Electric Company Technical Report, Salem, USA, pp.25-34.

George, F. Vander V. (2007): "Metallography Principles and Practice". ASM International, 4th Edition, Materials Park, Ohio, pp.410-426.

Ghosh, P. K., Robert, R. R. and Thomas, W. J. (2007): "The Development of a New Approach to Deoxidation of Molten Steel". Iron and Steel Technology, pp.96-104.

Hall, E. O., (1970): "Yield Point Phenomenon in Metals". Plenum Publishing Company, New York, 2ND Edition, pp. 49-72.

Hans, B. and Rolf, S. (1988): "Comparison of Production Costs for Hot Metal and Sponge Iron". Metallurgical Plant and Technology International, vol.22, No. 5, pp. 58-64.

Harry, B. and Rainer, O. (1996): "Advance Conceptss and Technologies for Bar Mills". Metallurgical Plant and Technology International, pp.66-79.

Helmult, C. (1992): "Mechanical Stability of Retained Austenite in Quenched and Tempered AISI 4340 Steel". Metallurgical Transaction A, vol.2, pp.216-242

Henkel and Pense (2002): "Structure and Properties of Engineering Materials". McGraw-Hill Series in Materials Science, 5th Edition, pp.189-191.

Higgins, R. A. (1985): "Properties of Engineering Materials". Hodder and Stoughton Educational, ELBS Edition, pp.56-58.

Hiroshi, K. (2007): "Production Technology of Iron and Steel in Japan". ISIJ International, vol.47, No.6, pp.773-794.

Honeycombe, R.W.K. and Bhadeshia, H.R.D. (1996): "Steels Microstructure and Properties". 2nd Edition, Weily, New York, pp.31-78.

Honeycombe, R.W.K. and Pickering, F.B. (1972): "Ferrite and Bainite in Alloy Steels". Metallurgical and Materials Transactions B, vol.3, No.3, pp.1099-1112.

Hong, X., Geoming, Y., Guomin, Z. and Jian, W. (2009): "Mathematical Model for Multi-Physical Process Coupling Analysis of Strip Hot Rolling". International Joint Conference on Computational Sciences and Optimisation, vol.1, pp.245-248.

Houbaert, Y., Petrov, R. and Barteri, M. (2005): "Study of Ferrite Grain Growth and Transformation Mechanisms". EUR, No.21430, pp.1-157.

Hurley, P.J. and Hodgson, P.D. (2001): "Formation of Ultra-fine Ferrite in the Hot Rolled Strip:Potential Mechanisms for Grain Refinement". Materials Science and Engineering A, vol.302, Issue 2, pp.206-214.

Inagaki, H. (1986): "Effect of Controlled Rolling on Ferrite-Pearlite Transformation in low Carbon-Niobium Steel". Z-Metal Limited, vol.77, No.1, pp.36-42.

Jeff, T., Jason, M.,, Ken, G., Reginald, D., Hans, J. and Alan E. (2007): "Structural Engineering with NiTi:: Basic Material Characterisation". Journal of Engineering Mechanics, vol.133, Issue 9, pp.1009-1018.

Jones, D. M., Watton, J. and Brown, K. J. (2006): "Prediction and Validation of Through Coil Final Mechanical Properties of High Strength Hot Rolled Coil Using Artificial Neural Networks". Journal of Ironmaking and Steelmaking, vol.33, No.4, pp.315-322.

Kamma, C.M. and Anagbo, R.E. (1989): "Role of Deformation on the Mechanical Treatment of Mild Steel". Proceedings of the 4th World Conference on Structural Analysis System, Paris, vol. 2, pp.448-456.

Kasuma, Y., Masaaki, T. and Tateshi, M. (1988): "A New Process for Hot Direct Charging". Journal of Steel Technology International, pp.231-232.

Kempter, M.H.A. (1979): "Materials for Engineers". Hodder and Stougthton Publshers, London, 3rd Edition, pp.48-61.

Kitamura, S. and Okohira, K. (1992): "Influence of Slag Composition and Temperature on Slag Foaming". ISIJ International, vol.32, No.6, pp.741-746.

Krauss, G. (1984): "Tempering and Structural Changes in Ferrous Martensites during Phase Transformation in Ferrous Alloys". Mander and Golden Eds., The Metallurgical Society, Warrendale PA, Pg.84.

Kumar, A., Singh, S.B. and Ray, K.K. (2008): "Influence of Bainite/Martensite Content on the Tensile Properties of Low Carbon Dual-Phase Steels". Materials Science and Engineering A., vol.474,Issue 1-2, pp.272-282.

Laasraoui, A. and Jonas, J.J. (2007): "Prediction of Temperature Distribution, Flow Stress and Microstructure during the Multipass Hot Rolling of Steel Plate and Strip". ISIJ International, vol.31, pp.95-105.

Lai, G.Y., Wood,W.E., Clark, R.A., Zackay, V.F. and Parker, E.R. (2007): "The Effect of Austenitising Temperature on the Microstructure and Mechanical Properties of As-Quenched 4340 Steel". Metallurgical and Meterials Transaction B, VOL.5, No.7, pp.1663-1670.

Liu, Y. and Lin, J. (2003): "Modelling of Microstructural Evolution in Multipass Hot Rolling". Journal of Materials Processing Technology, vol.143-144, pp.723-728.

Llwellyn, D.T. (1992): "Low Carbon Structural Steels". Journal of Steels, Metallurgy and Applications, pp.64-119.

Lotter, U. (1991): "Elaboration of Regression Equation to Describe the Transformation Behaviour during Thermo-mechanical Rolling". Commission of the European Committee Report on Construction Steeels, p.118.

Lundberg, S.E. (1997): "Roll-pass Design: Key Function in Control of Shape, Dimension and Mechanical Properties of Hot Rolled Propducts". Scandinavian Journal of Metallurgy, vol.26, No.3, pp.102-114.

Mamadou, B., Ndiaye, S.,Benard, C. and Ibrahim, K. (2009): "Evaluation and Improvement of the Quality of Senegalesse Reinforcing Steel Bars Produced from Metal Scraps". Journal of Materials and Design, vol.30, Issue 3, pp.804-809.

Markan, R.K. (2004): "Thermex Quenching and Tempering Technology". Article on Thermo-mechanical Steel Bars in India, pp.2-4.

Maunder, P.H.J. and Charles, J.A. (2006): "Behaviour of Non-Metallic Inclusions in a 0.2% Carbon Steel during Hot Rolling". Journal of Iron and Steel Institute, pp.705-715.

McQueen, H.J. and Ryan, N.D. (2002): "Constitutive Analysis of Hot Working". Journal of Materials Science and Engineering A, Vol.322, Issue 1-2, pp.43-63.

Ming-Chun Z., Ke, Y. and Yiying, S. (2002): "The Effects of Thermo-mechanical Control Process on Microstructures and Mechanical Properties of a Commercial Pipeline Steel". Materials Science and Engineering A, vol.335, Issue 1-2, pp.14-20.

Mudiare, E. (1977): "Process for Strengthening of Carbon Steels". Lasalle Steel Company, International Classification C210 952.

Mukhopadhway, A. and Sikdar, S. (2005): "Implementation of an On-Line Run-Out Table Model in a Hot Strip Mill". Journal of Materials Processing Technology, vol.169, Issue 2, pp.164-172.

Nikolaou, J., and Papadimitriou, G.D. (2004): "Comparative Microstructure and Mechanical Properties of Reinforcing Weldable Steel Produced by Various Processes (Tempcore, Microalloyed with vanadium and Work-hardened)". Constuction and Building Materials, vol.18, Issue 4, pp. 243-254.

NIS 117 (2004): "Standards of Steel Bars for Reinforcement of Concrete". Standards Organisation of Nigeria, Issue 3, pp.11-15.

Obikwelu, D.C.N. (1987): "Metallurgical Considerations in the Optimisation of Mechanical Properties of Rolled Products". Seminar Paper Presented at the Metallurgical and Research Department , Delta Steel Company, Aladja, Warri, Nigeria.

Oelmann and Davies (1983): "The Structure , Properties and Heat Treatment of Metals". Pitman Books, Great Britain, pp.54-57.

Ohtani, H., Okaguchi, S., Fujishiro, Y. and Ohmori, Y. (2007): "Morphology and Properties of Low Carbon Bainite". Metallurgical and Materials Transaction A, vol.21, No.3, pp.877-888.

Owen, G.W. and Knowles, P.R. (1992): "Steel Designer's Manual". Blackwell Scientific Publications, pp.845-846

Pauskar, P. and Shivpri, R. (2000): "Microstructure and Mechanics in the Modeling of Hot Rolling of Rods". CLEP Annals, Sweden.

Pereloma, E.V., Crawford, B.R. and Hodgson, P.D. (2001): "Strain-induced Precipitation Behaviour in Hot Rolled Strip Steel". Materials Science and Engineering, A299, pp.27-38.

Pickering F.B.(1958): "Influence of Mechanical Working on the Deformation of Non-Metallic Inclusions ". Journal of Iron and Steel Institute, vol.189, pp.149-158.

Philip, R. and Chapman, J.A. (1966): "Influence of Finish Rolling Temperature on the Mechanical Properties of some Commercial Steel Rolled to 13/16Diameter Bars". Japan Iron and Steel Institute (JISI), June 1966, p.615.

Prasun, D. and Shubharata, D. (2007): "Exploring the Effects of Chemical Composition in Hot Rolled Steel Product". Journal of Computational Materials Science, vol. 38, pp.671-677.

Pussegona, L.N. (1990): "Modeling Dynamic Softening Processes during Hot working". Metallurgical Transactions A, vol.21, pp.153-164.

Raja, B.V. Pal, N., Talwar, P.L. and Jayaswal, N.P. (2005): "The Use of Sponge Iron in Electric Arc Furnace (EAF)". Steel Times International, vol.29, No.3, pp.17-22.

Rajan, T.V., Sharma, C.P. and Sharma, A. (1988): "Heat Treatment Principles and Technique",.Prentice-Hall of India Limited, New Delhi, pp.47-238.

Raghavan, V. (2006): "Physical Metallurgy: Principles and Practice". Prentice-Hall of India, New Delhi, 2nd Edition, pp.65-99.

Randall, P. (2006): "Productivity Improvements in Steelmaking Process Control". Journal of Iron and Steel Technology, vol.3, No.1, January,2006, pp.31-42.

Rao, K.L. (1961): "Calculation, Design and Testing of Reinforced Concrete". Isaac Pitman and Sons Limited, London, p.97.

Ray, A., Mukerjei, D., Sen, S.K., Bhaltcharya, A., Dhua, S.K., Prasad, M.S., Barnerjie, N., Ppli, A.M. and Sahu, A.K. (1997): "Microstructure and Properties Thermodynamically Strengthened Reinforcement Bars: A Comparative Assessment of Plain-Carbon and Low –Alloy Steel Grades". Journal of Materials Engineering and Performance, vol.6, No.3, pp.335-343.

Respen, J. C. and Mario, E. (2001): "Rolled Steel Rod or Bar". Centre for Metallurgical Researches, USA, C22C 3500.

Rollason, E.C. (1973: "Metallurgy for Engineers". Edward Arnold Publishers, London, 4th Edition, pp.121-128.

Rudolf, K. and Lehert, W. (2002: "Hot Rolling in Ferrite Region". Scandinavian Journal of Metallurgy, vol. 9, Issue 4 pp. 215-258.

Ryoichi Takahashi (2001): "State of the Art in Hot Rolling Process Control". Journal of Control Engineering Practice, vol..9, Issue 9 September 2001, pp.987-993.

Sahajwalla, V., Castillejos, A.H. and Brimacombe, J.K. (2006): "Influence of Carbonaceous Materials in Slag-foaming Behaviour during EAF Steelmaking". Journal of Iron and Steel Technology, vol.3, No.2, pp..54-63.

Salvador, G. (2001): "Endless Rolling and Welding Process for Wire and Bar Mills". Metallurgical Plant and Technology International, No.3, pp.46-53.

Sameer, P., Praveen, P. and Rajiv, S. (2004): "Computational Modeling of Phase Transformation and Mechanical Properties during Cooling of Hot Rolled Rod". Journal of Materials Processing Technology, vol.150, Issue 1-2, pp.107-115.

Samuel, F.H. (1990): "Effect of Dynamic Recrystallisation on Microstructural Evolution duringip Rolling". ISIJ International, vol.30, pp.216-225.

Sangwoo, C. Y. and Peter, D. H. (2002): "Comparative Study of Microstructures and Mechanical Properties obtained by Bar and Plate Rolling". Journal of Materials Processing Technology, vol.124, Issue 3, pp.329-336.

Saroj, K.., Shih, J. and Satyanarayana, A. (2004): "Optimal Temperature Tracking for Accelerated Cooling Processes in Hot Rolling". Journal of Dynamics and Control, vol.7, No.4, pp.327-340.

Schaffer, J.P., Saxena, A., Antolovich, S.D., Sanders, T.H. and Warner, S. (1999): "The Science and Design of Engineering Materials". McGraw-Hill Company, 2nd Edition, pp.360-398.

Serajzadeh, S., Karimi, A. Taheri and Mucciardi (2002): "Prediction of Temperature Distribution in the Hot Rolling of Slabs". Modelling Simulation Materials Science Engineering, vol.10, pp.185-203.

Shinjiro, K., Jiro, H. and Takashi, I. (2003): "Kawasaki Steel Technical Report". No.48, March, 2003, pp.53-59.

Siamak Serajzadeh (2004): "Prediction of Dynamic Recrystallisation Kinetics during Hot Rolling". Modeling and Simulation in Materials Science and Enginering, vol.12, pp.1185-1200.

Sikdar, S. and John, S. (2007): "Effect of Water Jet Orientation and Other Controlling Parameters on Work Roll Temperature in a Hot Strip Mill". Journal of Materials and Manufacturing Processes, vol.22, No.1, pp.128-134.

Smallman, R.E. and Bishop, R.J. (1999): "Modern Physical Metallurgy and Materials Engineering". Butherworth Heinemann Publishers, 6th Edition, pp.209-211.

Tan, W., Liu, Z.Y., Wu, D. and Wang, G.D. (2008): "Artificial Neural Network (ANN) Modeling for the Energy Absorption of Hot Rolled Plates in Charpy Impact Test". Journal of Multidiscipline Modeling and Structures, vol.4, No.1, pp.37-46.

Tasuro, O., Hideo, K., Koji, A., Kishiro, T. and Manabu, K. (2001): "Microstructure and Mechanical Properties of Hot Rolled Bars for Machine Use". Nippon Steel Corporation USA, application No. 829741, pp.241-256.

Technical Bulletin, (1998): "Rolling Stocks Yield Evaluation". Standard Operating Procedures for Rolling Mill Plant. Issue 3, vol.2, pp.13-15.

Thackray, R., Steeper, M. and Ridal, K. (2009): "Influence of Rolling and Forging on Product Quality and Properties". Journal of Ironmaking and Steelmaking, vol.36, No.4, pp.265-272.

Thaller, G., Gerlinde, D. and Wolfgang, G. (2005): "Advanced Hot Strip and Plate Production of Steckel Mills". Metallurgical Plant and Technology International, No.1, Vol.28, pp.44-55.

Tietz, S.B. (1984): "Statutory Control of Civil Construction". Journal of Structural Engineers, London, vol.62A, No.12, pp.365-380.

Vijendra Singh (2004): "Heat Treatment of Metals". Standard Publishers, New Delhi, 2^{nd} Edition, pp.94-153.

Wusatowski, Z. (1969): "Fundamentals of Rolling". Pergamon Press Limited, London, pp.211-216.

Yada, H. (1987): "Accelerated Cooling of Rolled Steel". The Metallurgical Society, CIMM, Wimnipeg, MB Canada, pp.105-120.

Yasuya, O. (2007): "Bainitic Transformations in Extremely Low Carbon Steels". ISIJ International, vol.35, No.8, pp.962-968.

Yen, C.L. and Liu, Y.C. (1984): "Spread Characteristics of Passes in Rods and Bars Rolling". Journal of Technology and Training (Taiwan), vol.73, No.1, pp.20-35.

Young Kil (1988): "Quest for Competitive Clean Steel". Steel Technology International, pp.118-121.

Yu M. Lakhtin (1983): "Engineering Physical Metallurgy and Heat Treatment". Mir Publishers, Moscow, 2^{nd} Edition, pp.105-120.

Zambrano, P.C., Guerreo, M.P., Colas, R., and Ledue, L.A. (2001): "Microstructural Analysis of Hot Rolled Low-Carbon Steel Strip". Journal of Materials Characterisation, vol.47, Issue 3-4, November,2001, pp.275-282.

APPENDIX A – TENSILE RESULTS DATA OF AIR-COOLED SPECIMENS

Table A1 Tensile test results data analyses (Samples A, B and C)

A: Lo=23.14mm, A=19.46mm^2					B: Lo=23.53mm, A=20.11mm^2					C: Lo=23.36mm, A=19.32mm^2				
Ext. (mm)	Strain (e)	Load (KN)	True Strain ε	True Stress (MPa)	Ext. (mm)	Strain (e)	Load (KN)	True Strain ε	True Stress (MPa)	Ext. (mm)	Strain (e)	Load (KN)	True Strain ε	True Stress (MPa)
.517	.02	4.02	.02	210.7	.708	.03	5.01	.03	256.6	.258	.01	1.07	.01	56.0
.758	.03	5.04	.03	266.8	1.000	.04	6.50	.04	336.1	.325	.01	2.05	.01	107.2
.967	.04	6.02	.04	321.8	1.100	.05	7.02	.05	366.6	.400	.02	3.01	.02	158.9
1.18	.05	7.03	.05	379.4	1.390	.06	8.44	.06	444.9	.550	.02	4.08	.02	215.3
2.01	.09	8.00	.09	448.1	2.080	.09	9.01	.09	488.3	.750	.03	5.01	.03	267.1
2.767	.12	9.00	.11	518.0	3.000	.13	10.41	.12	585.0	.950	.04	6.01	.04	323.5
3.000	.13	9.22	.12	535.4	3.650	.16	11.00	.15	634.5	1.500	.06	7.22	.06	396.1
4.000	.17	9.76	.16	586.8	4.000	.17	11.21	.16	652.2	3.00	.13	8.67	.12	507.1
4.792	.21	9.88	.19	614.3	5.000	.21	11.51	.19	692.6	5.530	.24	9.42	.22	604.6
5.000	.22	9.87	.20	618.8	5.630	.24	11.55	.22	712.1	6.500	.28	9.31	.25	616.7
6.000	.26	9.21	.23	596.4	6.500	.28	11.44	.25	728.2	7.500	.32	8.61	.28	588.3
6.520	.28	8.08	.25	531.5	8.290	.35	9.05	.30	607.5	8.290	.35	6.87	.30	480.1
6.53	.28	4.64	.25	298.0	8.31	.35	5.39	.30	[illegible]	8.30	.36	3.82	.31	268.9
E=16551.38MPa					E=16117.08MPa					E=17347.13MPa				

Table A2 Tensile test results data analyses (Samples D and E)

D: Lo=26.21mm, A=20.67mm^2					E: Lo=23.37mm, A=20.19mm^2				
Ext. (mm)	Strain (e)	Load (KN)	True Strain ε	True Stress (MPa)	Ext. (mm)	Strain (e)	Load (KN)	True Strain ε	True Stress (MPa)
.533	.02	3.52	.02	179.8	.283	.01	2.03	.01	101.0
.733	.03	4.53	.03	225.8	.358	.02	3.03	.02	153.1
1.000	.04	5.89	.04	296.4	.700	.03	5.02	.03	256.1
1.200	.05	6.97	.05	354.1	1.000	.04	6.59	.04	339.5
1.500	.06	8.50	.06	435.9	1.270	.05	8.03	.05	417.6
1.725	.07	9.67	.07	500.5	2.000	.09	8.93	.09	482.1
2.500	.10	10.52	.10	559.8	3.000	.13	10.47	.12	586.0
3.500	.13	12.31	.12	672.9	4.000	.17	11.24	.16	651.3
4.000	.17	13.23	.16	748.8	5.250	.22	11.52	.20	696.1
5.890	.22	13.58	.20	801.5	6.000	.26	11.40	.23	711.4
5.940	.23	13.56	.21	806.9	7.000	.30	10.57	.26	680.6
8.250	.31	10.67	.27	676.2	7.670	.33	8.55	.29	563.3
8.26	.32	5.98	.28	381.9	7.68	.33	4.98	.29	328.1
E=13493.61MPa					E=16892.51MPa				

Table A3 Tensile test results data analyses (Samples F and G)

F: Lo=24.92mm, A=21.73mm^2					G: Lo=22.38mm, A=19.71mm^2				
Ext. (mm)	Strain (e)	Load (KN)	True Strain ε	True Stress (MPa)	Ext. (mm)	Strain (e)	Load (KN)	True Strain ε	True Stress (MPa)
.283	.01	2.13	.01	99.0	.300	.01	2.13	.01	157.4
.425	.02	4.03	.02	189.2	.442	.02	4.03	.02	260.8
.808	.03	6.02	.03	285.3	.583	.03	6.02	.03	315.1
1.000	.04	7.02	.04	336.0	.758	.03	7.02	.03	367.4
2.000	.08	8.36	.08	414.7	1.000	.04	8.36	.04	442.2
3.000	.12	9.67	.11	498.4	1.183	.05	9.67	.05	499.2
4.000	.16	10.37	.15	553.6	2.040	.09	10.37	.09	553.6
5.000	.20	10.71	.18	591.5	3.000	.13	10.71	.12	648.4
6.260	.25	10.83	.22	623.0	5.000	.22	10.83	.20	749.6
7.000	.28	10.79	.25	635.5	6.000	.27	10.79	.24	773.2
8.000	.32	10.63	.28	645.7	7.000	.31	10.63	.27	745.8
10.420	.42	7.42	.35	484.9	7.925	.35	7.42	.30	624.6
10.43	.42	4.45	.35	290.8	7.94	.35	5.03	.30	344.5
E=17612.01MPa					E=19157.85MPa				

APPENDIX B: MATLAB DATA SCHEDULE FOR STRESS-STRAIN BEHAVIOUR OF CONVENTIONAL AIR-COOLED SPECIMENS

```
x=[0.02,0.03,0.04,0.05,0.09,0.11,0.12,0.16,0.19,0.2,0.23,0.25,0.25];
y=[210.7,266.8,321.8,379.4,448.1,518,535.4,586.8,614.3,618.8,596.4,531.5,298];
x1=[0.03,0.04,0.05,0.06,0.09,0.12,0.15,0.16,0.19,0.22,0.25,0.28,0.3];
y1=[256.6,336.1,366.6,444.9,488.3,585,634.5,652.2,692.6,712.1,728.2,607.5,361.8];
x2=[0.01,0.01,0.02,0.02,0.03,0.04,0.06,0.12,0.22,0.25,0.28,0.3,0.31];
y2=[56,107.2,158.9,215.3,267.1,323.5,396.1,507.1,604.6,616.7,588.3,480.1,268.9];
x3=[0.02,0.03,0.04,0.05,0.06,0.07,0.1,0.12,0.16,0.2,0.21,0.27,0.28];
y3=[179.8,225.8,296.4,354.1,435.9,500.5,559.8,672.9,748.8,801.5,806.9,676.2,381.9];
x4=[0.01,0.02,0.03,0.04,0.05,0.09,0.12,0.16,0.2,0.23,0.26,0.29,0.29];
y4=[101,153.1,256.1,339.5,417.6,482.1,586,651.3,696.1,711.4,680.6,563.3,328.1];
x5=[0.01,0.02,0.03,0.04,0.08,0.11,0.15,0.18,0.22,0.25,0.28,0.35,0.35];
y6=[157.4,260.8,315.1,367.4,442.2,499.2,553.6,648.4,749.6,773.2,745.8,624.6,344.5];
y5=[99,189.2,285.3,336,414.7,498.4,553.6,591.5,623,635.5,645.7,484.9,290.8];
x6=[0.01,0.02,0.03,0.03,0.04,0.05,0.09,0.12,0.2,0.24,0.27,0.3,0.3];
plot(x,y,x1,y1,x2,y2,x3,y3,x4,y4,x5,y5,x6,y6)
```

APPENDIX C TRUE STRESS-STRAIN DATA OF SPRAY-QUENCHED SPECIMENS AT VARYING AUSTENITISING TEMPERATURES

Table C1 True stress-strain at 800^{O}C

Water-spray duration (s)													
5		10		15		20		25		30		40	
Strain	Stress	Straio	Stress	Strain	Stress	Strain	Stress	Strain	Stress	Strain	Stress	Strain	Stress
0.012	161.1	0.026	159.3	0.014	134.7	0.017	80.4	0.070	107.6	0.027	147.9	0.016	80.9
0.019	308.3	0.047	638.7	0.018	257.8	0.027	271.0	0.083	326.6	0.032	262.1	0.019	162.3
0.035	661.9	0.050	709.9	00.026	406.0	0.033	361.8	0.092	494.4	0.044	405.9	0.023	325.8
0.045	842.8	0.063	685.5	0.031	509.0	0.043	446.0	0.093	508.3	0.050	461.0	0.031	398.3
0.050	884.5	0.069	748.4	0.040	633.0	0.050	553.0	0.117	490.8	0.055	435.0	0.034	340.3
0.078	1008.2	0.135	1015.0	0.079	687.7	0.059	524.9	0.131	560.8	0.089	509.7	0.040	360.5
0.095	1061.7	0.176	1110.6	0.110	796.4	0.087	576.3	0.191	693.1	0.135	627.6	0.120	538.9
0.131	981.2	0.218	1173.6	0.153	8887.3	0.113	614.4	0.218	732.2	0.205	704.0	0.172	614.1
0.154	893.1	0.305	1158.9	0.191	939.2	0.140	604.5	0.247	724.1	0.255	694.2	0.201	596.9
0.176	775.4	0.329	1015.4	0.248	825.6	0.162	505.9	0.252	506.8	0.291	556.1	0.237	427.1

Table C2 True stress-strain at 820^{O}C

Water-spray duration (s)													
5		10		15		20		25		30		40	
Strain	Stress	Strain	Stress	Strain	Stress	Strain	Stress	Strain	Stress	Strain	Stress	Strain	Stress
0.016	101.9	0.018	51.7	0.018	50.2	0.017	95.8	0.019	46.9	0.016	49.2	0.018	75.1
0.024	205.3	0.023	207.7	0.029	217.0	0.027	290.2	0.024	188.5	0.020	148.1	0.024	166.9
0.030	413.0	0.032	311.9	00.31	305.30	0.033	377.9	0.031	284.7	0.022	194.9	0.029	260.9
0.043	554.7	0.044	435.1	0.039	410.7	0.043	395.4	0.036	381.8	0.026	183.7	0.037	369.5
0.064	598.5	0.068	407.1	0.044	397.2	0.049	384.8	0.041	352.0	0.043	227.4	0.048	335.6
0.124	726.3	0.136	438.9	0.070	436.5	0.068	441.0	0.060	372.4	0.091	304.2	0.085	464.2
0.180	784.8	0.194	586.0	0.134	569.2	0.138	565.1	0.107	500.9	0.147	348.6	0.123	499.6
0.215	862.4	0.228	638.7	0.179	607.7	0.165	591.70	0.172	555.9	0.169	363.9	0.164	540.1
0.247	840.5	0.262	619.5	0.195	602.7	0.201	560.1	0.203	545.2	0.204	356.1	0.192	525.7
0.268	664.9	0.252	346.3	0.242	456.6	0.213	377.7	0.230	457.3	0.233	248.0	0.220	442.5

Table C3 True stress-strain at 840^{O}C

Water-spray duration (s)													
5		10		15		20		25		30		40	
Strain	Stress	Strain	Stress	Strain	Stress	Strain	Stress	Strain	Stress	Strain	Stress	Strain	Stress
0.019	93.4	0.016	44.4	0.019	44.8	0.017	44.6	0.018	95.1	0.019	96.4	0.019	82.7
0.022	187.4	0.024	178.9	0.022	89.9	0.026	179.9	0.025	191.6	0.026	194.0	0.029	250.7
0.033	379.3	0.037	362.6	00.31	113.4	0.037	373.2	0.031	376.1	0.031	383.2	0.033	335.9
0.041	508.8	0.043	405.7	0.036	182.5	0.042	384.1	0.040	389.2	0.049	387.2	0.036	373.7
0.066	543.5	0.051	382.2	0.052	389.1	0.054	398.1	0.062	407.7	0.095	488.9	0.045	354.6
0.097	622.5	0.174	442.1	0.067	404.5	0.094	490.5	0.093	492.1	0.154	562.8	0.059	364.0
0.128	670.9	0.142	553.8	0.078	386.2	0.124	526.0	0.149	564.5	0.169	584.3	0.096	456.9
0.174	743.2	0.173	589.7	0.140	536.3	0.158	563.8	0.177	541.2	0.183	574.1	0.147	516.1
0.186	727.6	0.207	454.6	0.212	617.3	0.194	538.6	0.183	534.3	0.210	565.9	0.156	507.8
0.200	699.4	0.256	465.6	0.284	453.6	0.215	467.4	0.191	466.1	0.228	476.9	0.181	473.7

Table C4 True stress-strain at 860^{O}C

Water-spray duration (s)													
5		10		15		20		25		30		40	
Strain	Stress	Strain	Stress	Strain	Stress	Strain	Stress	Strain	Stress	Strain	Stress	Strain	Stress
0.012	45.1	0.020	95.0	0.022	97.4	0.021	104.0	0.017	101.3	0.021	86.6	0.014	48.9
0.019	182.0	0.022	190.3	0.028	195.9	0.026	209.1	0.019	202.0	0.031	349.8	0.019	147.3
0.025	274.7	0.037	286.9	00.35	296.1	0.032	315.7	0.027	305.4	0.037	394.4	0.029	218.2
0.048	487.0	0.037	422.4	0.045	41.7	0.037	394.5	0.032	394.2	0.045	368.2	0.031	178.3
0.049	457.7	0.038	387.0	0.053	391.7	0.040	365.9	0.039	372.1	0.056	403.8	0.050	212.7
0.079	507.4	0.65	436.7	0.080	441.1	0.060	411.2	0.065	417.7	0.066	416.7	0.066	241.9
0.114	556.2	0.119	534.7	0.117	542.5	0.117	538.2	0.095	485.1	0.128	529.9	0.096	297.1
0.118	550.7	0.141	576.7	0.162	592.1	0.160	590.1	0.130	535.2	0.166	586.2	0.148	340.0
0.148	518.5	0.153	551.6	0.188	577.9	0.205	568.8	0.155	531.9	0.186	579.5	0.171	332.1
0.161	451.4	0.191	493.7	0.239	471.0	0.240	459.1	0.180	431.5	0.226	463.2	0.210	132.4

Table C5 True stress-strain at 880^{O}C

Water-spray duration (s)													
5		10		15		20		25		30		40	
Strain	Stress	Strain	Stress	Strain	Stress	Strain	Stress	Strain	Stress	Strain	Stress	Strain	Stress
0.016	97.6	0.027	95.6	0.019	107.2	0.024	89.8	0.017	96.5	0.018	99.7	0.021	82.9
0.020	195.9	0.031	192.0	0.027	216.1	0.031	180.8	0.023	194.2	0.022	200.2	0.033	251.9
0.028	291.1	0.037	289.9	00.38	421.9	0.044	366.5	0.033	357.9	0.028	302.1	0.044	370.5
0.036	458.0	0.041	388.1	0.040	383.3	0.051	387.4	0.049	350.8	0.034	324.4	0.051	341.7
0.064	557.8	0.045	487.0	0.065	421.0	0.062	397.0	0.054	390.9	0.041	379.3	0.063	347.6
0.091	613.5	0.065	556.4	0.095	497.6	0.080	427.3	0.057	357.4	0.043	358.9	0.119	473.2
0.109	593.1	0.096	645.8	0.154	577.1	0.154	555.1	0.131	534.0	0.065	397.1	0.200	559.7
0.123	564.7	0.161	763.3	0.176	605.5	0.200	601.8	0.162	559.6	0.138	535.8	0.257	561.7
0.138	509.0	0.176	756.5	0.210	591.4	0.255	599.5	0.190	550.8	0.155	514.8	0.289	501.4
0.150	444.7	0.192	628.2	0.251	405.1	0.307	467.0	0.215	466.2	0.175	302.9	0.306	436.2

Table C6 True stress-strain at 900^{O}C

Water-spray duration (s)													
S		10		15		20		25		30		40	
Strain	Stress	Strain	Stress	Strain	Stress	Strain	Stress	Strain	Stress	Strain	Stress	Strain	Stress
0.018	85.7	0.014	45.8	0.017	47.3	0.017	47.3	0.017	45.9	0.017	42.6	0.017	45.4
0.028	259.7	0.019	92.1	0.019	94.9	0.019	94.9	0.022	135.5	0.023	86. 1	0.019	119.0
0.033	348.3	0.022	184.6	00.23	190.5	0.026	191.1	0.025	230.8	0.025	172. 6	0.023	182.8
0.037	419.6	0.027	278.3	0.0373	384.4	0.030	287.7	0.037	370.1	0.035	340. 5	0.025	228.9
0.049	495.2	0.048	411.4	0.050	362.1	0.037	372.0	0.067	294.5	0.066	356. 1	0.027	326.5
0.095	556.7	0.051	389.2	0.082	454.6	0.096	378.8	0.129	429.1	0.096	417. 2	0.032	381.4
0.108	575.2	0.067	444.2	0.128	529.3	0.126	419.2	0.194	457.8	0.127	473. 6	0.095	368.5
0.126	572.0	0.129	587.0	0.183	583.7	0.163	447.3	0.216	456.8	0148	493. 0	0.152	427.3
0.154	506.1	0.166	630.7	0.214	583.2	0.183	434.8	0.256	434.8	0.156	492. 7	0.182	412. 7
0.176	407.1	0.247	489.0	0.244	472.6	0.226	344.9	0.285	344.9	0.184	443. 3	0.205	341. 0

Table C7 True stress-strain at 1000^{O}C

Water-spray duration (s)													
5		10		15		20		25		30		40	
Strain	Stress	Strain	Stress	Strain	Stress	Strain	Stress	Strain	Stress	Strain	Stress	Strain	Stress
0.020	47.5	0.024	86.9	0.018	93.4	0.015	49.9	0.019	45.2	0.016	42.5	0.015	42.7
0.032	192.4	0.030	174.7	0.024	187.9	0.021	200.8	0.026	181.9	0.023	171.0	0.025	172.6
0.038	290.2	0.034	263.4	0.029	283.1	0.027	302.9	0.038	276.3	0.030	258.5	0.028	259.7
0.046	414.9	0.043	398.0	0.033	379.3	0.029	398.5	0.047	376.3	0.037	369.9	0.048	368.2
0.053	385.2	0.059	369.0	0.0050	378.3	0.049	356.2	0.067	375.3	0.040	349.8	0.057	356.7
0.079	423.1	0.115	523.4	0.066	401.1	0.094	486.3	0.120	529.5	0.079	452.2	0.095	472.4
0.128	542.6	0.151	582.0	0.097	493.1	0.125	557.0	0.165	597.0	0.116	515.3	0.126	525.2
0.192	613.7	0.205	626.7	0.146	545.9	0.148	575.3	0.192	588.8	0175	589.4	0.170	583.0
0.250	585.8	0.251	579.8	0.157	544.0	0.167	569.5	0.209	560.2	0.220	572.2	0.210	555.9
0.278	472.3	0.313	483.8	0.205	423.2	0.206	455.1	0.237	460.4	0.256	357.4	0.239	449.3

Table C8 Impact energy of air-cooled (as-rolled) test specimens

Specimen number	**1**	**2**	**3**	**4**	**5**	**6**	**7**
Impact energy (J)	81.9	80.7	81.5	82.0	78.4	79.6	80.3

APPENDIX D MECHANICAL PROPERTY DATA OF SPRAY-QUENCHED SPECIMENS

Table D1 Yield strength property of test specimens

Cooling rate $^0C/s$	Yield Strength (MPa)/Temperature (^0C)						
	800	820	840	860	880	900	1000
118	842.8	554.2	508.8	487.0	458.0	419.6	414.9
65	709.9	487.0	435.1	422.4	411.4	405.7	398.0
47	633.0	425.7	417.3	410.7	404.5	384.4	379.3
36	553.0	421.9	398.5	398.1	395.4	394.5	372.0
28	508.3	397.0	394.2	389.2	381.8	371.6	370.1
24	461.0	394.4	390.9	382.2	369.9	340.5	218.2
18	398.3	379.3	373.7	369.5	368.2	326.5	194.9

Table D2 Stiffness variations of test specimens

Cooling rate $^0C/S$	Modulus (MPa)/ Temperature (^0C)						
	800	820	840	860	880	900	1000
118	18321.7	12606.8	12095.2	9938.8	12378.4	11042.1	8827.7
65	13919.6	11156.4	9220.5	11115.8	10587.0	10034.1	9045.5
47	15439.0	10267.5	5862.3	9080.4	10817.9	10115.8	11155.9
36	10843.1	8936.4	7108.9	10302.6	6203.7	9789.5	13741.4
28	5186.7	10318.9	9492.7	11945.5	6980.4	9739.5	7839.6
24	9039.2	8859.1	12361.1	10378.9	9031.0	9458.3	9734.2
18	6623.1	9723.7	10100.0	7524.1	8233.3	12092.6	8980.5

TableD3 Impact energy absorbed at varying cooling rates and temperature by test specimens

Cooling rate $^0C/S$	Impact energy (J) / Temperature (^0C)						
	800	820	840	860	880	900	1000
118	94.8	99.1	100.2	105.7	109.3	110.0	111.0
65	85.2	89.4	93.7	96.0	98.7	103.2	109.2
47	79.6	87.2	92.6	94.9	96.8	101.4	106.5
36	78.3	86.9	91.7	92.5	95.1	100.2	105.4
28	76.9	84.6	90.4	91.2	93.7	98.6	101.2
24	76.2	83.8	88.5	89.3	91.4	97.1	98.7
18	75.7	81.7	86.8	87.6	90.5	95.3	96.8

Table D4 Plastic strain variations of test specimens

Cooling rate $^0C/S$	Strain ($x\ 10^{-3}$) Temperature (^0C)						
	800	820	840	860	880	900	1000
118	176	268	200	161	150	176	278
65	329	262	256	191	192	247	313
47	248	242	282	239	251	244	205
36	162	213	215	240	307	226	206
28	252	230	191	180	215	285	237
24	291	233	228	226	175	184	256
18	237	220	181	210	306	205	239

Table D5 Hardness of spray-quenched test specimens

Cooling rate ^{0}C/S	Hardness value (HRB)/ Temperature (^{0}C)						
	800	820	840	860	880	900	1000
118	108.5	103.1	98.3	87.1	91.4	88.6	86.8
65	110.8	93.6	90.5	89.4	99.3	92.1	92.7
47	105.1	91.8	92.3	90.0	91.0	89.8	86.2
36	91.6	90.7	87.4	90.6	91.8	77.6	89.1
28	97.0	87.4	88.3	86.1	87.9	78.5	90.6
24	96.2	86.8	89.1	89.6	85.7	81.9	90.8
18	91.8	86.2	84.3	62.0	87.6	74.6	89.7

UNIVERSITY OF LAGOS